Journal of South American Earth Sciences 79 (2017) 111–136

Contents lists available at ScienceDirect

Journal of South American Earth Sciences

journal homepage: www.elsevier.com/locate/jsames

The Nahuel Niyeu basin: A Cambrian forearc basin in the eastern North Patagonian Massif

Gerson A. Greco [a, *], Santiago N. González [a], Ana M. Sato [b], Pablo D. González [a], Miguel A.S. Basei [c], Eduardo J. Llambías [b], Ricardo Varela [b]

[a] Instituto de Investigación en Paleobiología y Geología (UNRN-CONICET), Av. Julio A. Roca 1242, R8332-EXZ General Roca, Río Negro, Argentina
[b] Centro de Investigaciones Geológicas (UNLP-CONICET), Diagonal 113 N° 275, B1904-DPK La Plata, Buenos Aires, Argentina
[c] Centro de Pesquisas Geocronológicas (Instituto de Geociências, USP), Rua do Lago 562, CEP 05508-080 São Paulo, SP, Brazil

ARTICLE INFO

Article history:
Received 10 February 2017
Received in revised form
11 July 2017
Accepted 21 July 2017
Available online 25 July 2017

Keywords:
Southwestern Gondwana margin
U–Pb geochronology
Pampean orogen
El Jagüelito Formation
Mina Gonzalito Complex
Nahuel Niyeu Formation

ABSTRACT

Early Paleozoic basement of the eastern North Patagonian Massif includes low- and high grade metamorphic units, which consist mainly of alternating paraderived metamorphic rocks (mostly derived from siliciclastic protoliths) with minor intercalations of orthoderived metamorphic rocks. In this contribution we provide a better understanding of the tectonic setting in which the protoliths of these units were formed, which adds to an earlier suggested idea. With this purpose, we studied the metasedimentary rocks of the low-grade Nahuel Niyeu Formation from the Aguada Cecilio area combining mapping and petrographic analysis with U–Pb geochronology and characterization of detrital zircon grains. The results and interpretations of this unit, together with published geological, geochronological and geochemical information, allow us to interpret the sedimentary and igneous protoliths of all metamorphic units from the massif as formed in a forearc basin at ~520–510 Ma (Nahuel Niyeu basin). It probably was elongated in the ~NW–SE direction, and would have received detritus from a proximal source area situated toward its northeastern side (present coordinates). The basin might be related to an extensional tectonic regime. Most likely source rocks were: (1) 520–510 Ma, acidic volcanic rocks (an active magmatic arc), (2) ~555 –>520 Ma, acidic plutonic and volcanic rocks (earlier stages of the same arc), and (3) latest Ediacaran-Terreneuvian, paraderived metamorphic rocks (country rocks of the arc). We evaluate the Nahuel Niyeu basin considering the eastern North Patagonian Massif as an autochthonous part of South America, adding to the discussion of the origin of Patagonia.

1. Introduction

Early Paleozoic basement of the eastern North Patagonian Massif typically exhibits low- and high-grade metamorphic units; Cambrian–Ordovician granitoid plutons also belong to the basement. The metamorphic units consist mainly of alternating paraderived metamorphic rocks with minor intercalations of orthoderived metamorphic rocks, the former mostly derived from siliciclastic protoliths, whereas the latter derived from pyroclastic, volcanic and subvolcanic protoliths. Detrital zircon studies revealed Cambrian maximum depositional ages and an older Gondwanan provenance for the siliciclastic protoliths of the metamorphic units (Pankhurst et al., 2006; Naipauer et al., 2010; Martínez Dopico et al., 2011; Rapalini et al., 2013; Greco et al., 2014, 2015). Moreover, petrographical, geochronological and geochemical studies suggest that both the siliciclastic and igneous protoliths were related to a convergent continental margin associated with active arc magmatism (Cagnoni et al., 1993; Giacosa, 1997; Dalla Salda et al., 2003a; Pankhurst et al., 2006; González et al., 2013; Greco et al., 2015). Furthermore, Greco et al. (2015) considered the sedimentary and igneous protoliths of the metamorphic units as formed in a basin associated with this tectonic setting, during the Early Cambrian. Other interpretations suggest a collisional continental margin as tectonic setting for protoliths of the metamorphic units (Ramos and Naipauer, 2014).

Maximum depositional ages together with stratigraphic, structural, metamorphic and U–Pb age constraints indicate a

* Corresponding author. Instituto de Investigación en Paleobiología y Geología, Universidad Nacional de Río Negro, Av. Julio A. Roca 1242, R 8332 EXZ General Roca, Río Negro, Argentina.
E-mail addresses: ggreco@unrn.edu.ar, gersongreco@gmail.com (G.A. Greco), sgonzalez@unrn.edu.ar (S.N. González), sato@cig.museo.unlp.edu.ar (A.M. Sato), pdgonzalez@unrn.edu.ar (P.D. González), baseimas@usp.br (M.A.S. Basei), llambias@cig.museo.unlp.edu.ar (E.J. Llambías), ricardovarela47@yahoo.com.ar (R. Varela).

http://dx.doi.org/10.1016/j.jsames.2017.07.009
0895-9811/

Cambrian–Ordovician main evolution for the basement, including deposition of sedimentary protoliths, regional metamorphism and deformation, and plutonism; Permian tectonism associated with metamorphism and magmatism also affected the basement (Caminos and Llambías, 1984; Chernicoff and Caminos, 1996a, 1996b; Giacosa, 1999; Giacosa and Paredes, 2001; von Gosen, 2002, 2003; González et al., 2002, 2011b; Pankhurst et al., 2006; Gozalvez, 2009b; Rapalini et al., 2013; Varela et al., 2014; Pankhurst et al., 2014; Greco et al., 2015).

The geologic evolution of the basement rocks of the eastern North Patagonian Massif are related to the origin of Patagonia and its evolution in the southern margin of Gondwana during the Paleozoic. At this respect, several alternatives have been postulated. One main alternative considers all Patagonia as an allochthonous terrane accreted to the southwestern margin of Gondwana during the late Paleozoic (Ramos, 1984, 2008). This alternative was reinforced by contributions that have argued for an Antarctic-Patagonia connection in the early Paleozoic (González et al., 2011b; Ramos and Naipauer, 2014). Other main alternative suggest that the Pampean (Neoproterozoic–Middle Cambrian) and Famatinian (Late Cambrian–Devonian) orogens from Northwestern Argentina and Eastern Sierras Pampeanas regions might stretch southward into northern Patagonia, considering the North Patagonian Massif as an autochthonous part of South America (Rapela and Pankhurst, 2002; Pankhurst et al., 2003, 2006; Gregori et al., 2008; Rapalini et al., 2013). Further studies supported this continuity, but considered the North Patagonian Massif as a parautochtonous block detached from South America during the early-middle Paleozoic, opening a small ocean that subsequently was closed in the late Paleozoic (Rapalini et al., 2010; López de Luchi et al., 2010; Martínez Dopico et al., 2011; Pankhurst et al., 2014). Other contributions consider all Patagonia as an autochthonous part of South America (Forsythe, 1982; Varela et al., 1991; Dalla Salda et al., 1992). All alternatives are a current topic of discussion.

The aim of this study is to provide a better understanding of the tectonic setting in which the sedimentary and igneous protoliths of the metamorphic units from the eastern North Patagonian Massif were formed. It has implications in the tectonic evolution of northern Patagonia during the early Paleozoic and adds to the discussion of its origin.

With the above purpose, we map and describe the paraderived metamorphic rocks of the low-grade Nahuel Niyeu Formation from the Aguada Cecilio outcrops, Río Negro province - Argentina (Figs. 1b and 2), including their relict primary features. In addition, we determine LA–MC–ICPMS U–Pb ages and characteristics of detrital zircon grains from three representative metasandstones. The results, together with the published geochronological, petrographical and geochemical data, allow us to characterize the sedimentary protoliths of the Nahuel Niyeu Formation from the point of view of depositional age, maturity and source rocks. From this characterization, we compare this unit with other metamorphic units of the eastern North Patagonian Massif, in order to contribute to regional comparisons from the perspective of the protoliths. Our regional analysis throughout the eastern North Patagonian Massif essentially agrees with the above depicted idea of Greco et al. (2015) regarding to the basin and timing in which the sedimentary and igneous protoliths of the metamorphic units were formed. Besides, we interpret the position of the source area of the basin, the type of basin and the associated tectonic regime. Additionally, we evaluate the basin considering the idea of the North Patagonian Massif as an autochthonous block, adding to the discussion of the origin of Patagonia.

The geologic time scale used in this contribution is the Geologic Time Scale v4.0 of the Geological Society of America (Walker et al., 2012). The approximate correspondence with the following traditional division of the Cambrian Period into early (Terreneuvian and Epoch 2), middle (Epoch 3) and late (Furongian) is based on Babcock and Peng (2007) and Peng et al. (2012).

2. Regional geology of the eastern North Patagonian Massif

Early Paleozoic basement units of the eastern North Patagonian Massif crop out in three main areas, depicted in Fig. 1b (Nahuel Niyeu–Aguada Cecilio area), 1c (Mina Gonzalito–Sierra Pailemán area) and 1d (Sierra Grande area). Small and scattered basement outcrops are also located in the areas of El Gualicho salt lake and south of Las Grutas (Fig. 1).

The Nahuel Niyeu Formation (Caminos, 1983) crops out in the Nahuel Niyeu–Aguada Cecilio area (Fig. 1b). It consists mainly of alternating beds of metagreywackes, phyllites and slates, and minor intercalations of metaigneous rocks (Núñez et al., 1975; Caminos, 1983, 2001; Cagnoni et al., 1993; Chernicoff and Caminos, 1996a; Giacosa, 1999; Greco et al., 2015). SHRIMP U–Pb detrital zircon data indicate maximum depositional ages of 515–507 Ma for the siliciclastic protoliths (Pankhurst et al., 2006; Rapalini et al., 2013). A SHRIMP U–Pb zircon age of 513.6 Ma constrains the timing of magmatic crystallization of the metaigneous rocks (Greco et al., 2015). Fabric orientation in the Aguada Cecilio area is WNW–ESE and given by parallel structures associated with a main M_1 regional metamorphism (greenschist facies, biotite zone) of early Paleozoic age and a subsequent M_2 regional metamorphism (greenschist facies, chlorite zone) of Permian age (Greco et al., 2015). The NE–SW fabric orientation between Valcheta and Nahuel Niyeu (Fig. 1b) was linked to Permian or younger tectonism (von Gosen, 2003; Greco et al., 2015). Granitoid plutons belonging to the Ordovician Punta Sierra Plutonic Complex (i.e. Valcheta Pluton) and equivalent microgranodiorite dikes intrude the Nahuel Niyeu Formation (Caminos, 1983, 2001; Busteros et al., 1998; López de Luchi et al., 2008; Gozalvez, 2009b; Rapalini et al., 2013; Greco et al., 2015). Scattered outcrops of metagreywackes, schists and hornfels from the area of El Gualicho salt lake (Fig. 1) were considered as belonging to the Nahuel Niyeu Formation because of similar lithology (Caminos and Llambías, 1984).

The Yaminué Complex (Caminos, 1983) of medium to high metamorphic grade crops out in the western side of the Nahuel Niyeu–Aguada Cecilio area (Fig. 1b). It contains foliated granitoids and leucogranites, heterogeneously foliated porphyroid granodiorites (Tardugno Granodiorite), with minor paragneisses, schists, amphibolites and marbles (Caminos, 1983, 2001; Caminos and Llambías, 1984; Chernicoff and Caminos, 1996b). Conventional and SHRIMP U–Pb zircon ages include Terreneuvian (Tardugno Granodiorite), Ordovician and Permian-Triassic magmatism (Basei et al., 2002; Rapalini et al., 2013; Chernicoff et al., 2013; Pankhurst et al., 2014; Martínez Dopico et al., 2016). A SHRIMP U–Pb detrital zircon study provides a Carboniferous maximum depositional age from a biotitic paragneiss-schist (Chernicoff et al., 2013). The Tardugno Granodiorite is juxtaposed against the Nahuel Niyeu Formation by a late Paleozoic SE-directed reverse fault (von Gosen, 2003), whereas the remaining dated outcrops are located west of the limits of Fig. 1.

The Mina Gonzalito Complex (Giacosa, 1987) crops out in the Mina Gonzalito–Sierra Pailemán area (Fig. 1c). It mainly includes alternating layers of paragneisses, schists and migmatites, and minor intercalations of marbles and amphibolites. A granodioritic orthogneiss and syntectonic leucogranites are considered as part of the complex. SHRIMP and LA–ICPMS U–Pb detrital zircon data indicate maximum depositional ages of 515 Ma (sample GNZ-068, Greco et al., 2014) and 540–535 Ma (sample GON-14, Pankhurst et al., 2006) for the siliciclastic protoliths of the paragneisses (Fig. 1c), whereas strontium isotopic studies indicate ca. 550–510

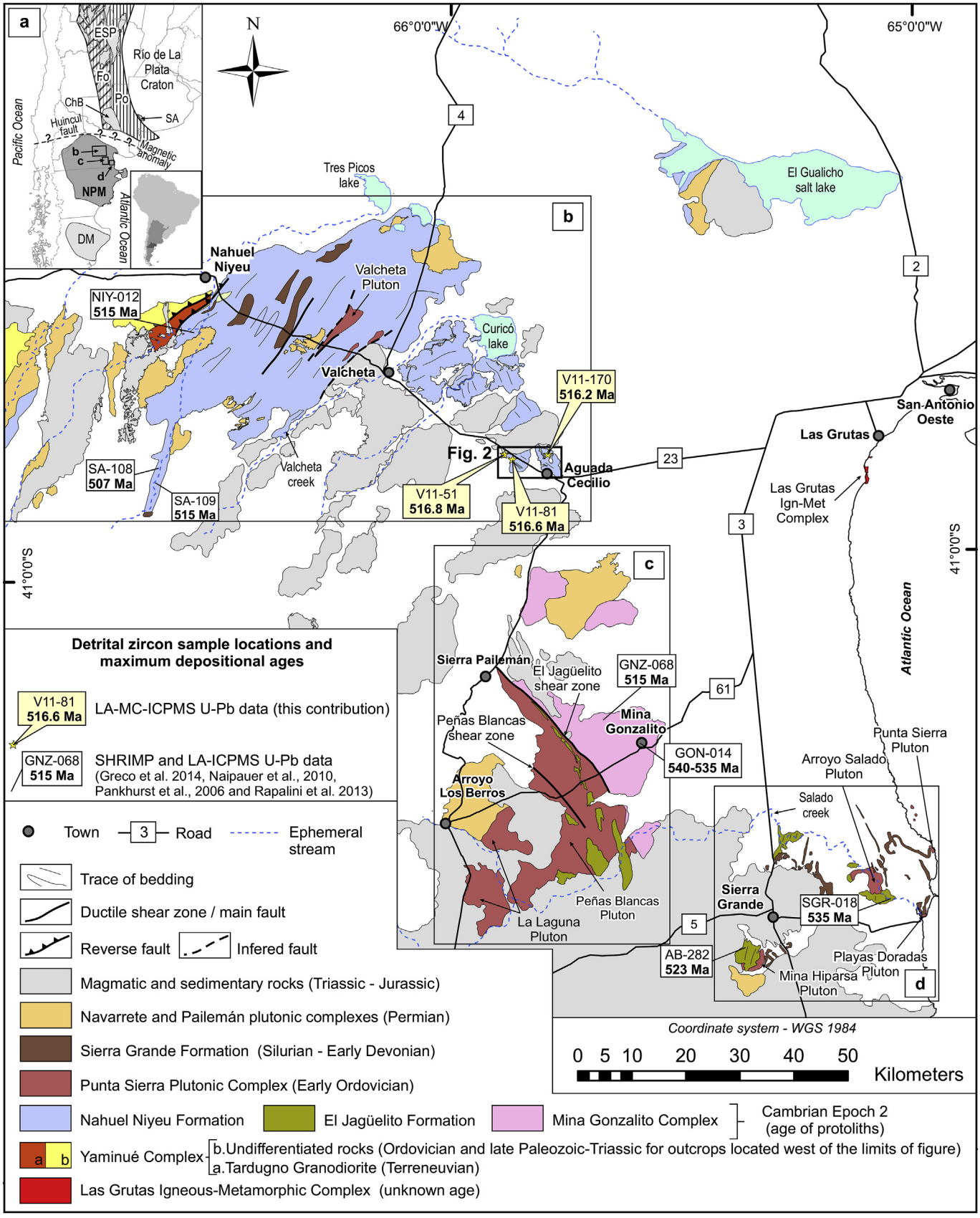

Fig. 1. Geology of the eastern North Patagonian Massif, based on the geological maps of Busteros et al. (1998), Caminos (2001) and Martínez et al. (2001), modified after Greco et al. (2015). Age of the geological units is based on cited works in the text. (a) Regional situation of the North Patagonian Massif (NPM) in the context of South America and Argentina compiled and adapted after Sato et al. (2003) and Varela et al. (2011b). Morphostructural regions (NPM: North Patagonian Massif; DM: Deseado Massif; ESP: eastern Sierras Pampeanas; SA: Sierras Australes) and Pampean (Po) and Famatinian (Fo) orogens are indicated, as well as the potential suture of the Patagonia terrane in dotted line (Ramos, 2008, 1984). To the west of the Río de la Plata craton was developed the Pampean orogen (Neoproterozoic to Middle Cambrian) and its western boundary was then affected by magmatism, deformation and regional metamorphism of the Famatinian orogen (Late Cambrian to Devonian). Southwestern limit of the Rio de la Plata Craton was determined according to Pángaro and Ramos (2012). (b–d) Simplified regional geology of the Nahuel Niyeu-Aguada Cecilio (b), Mina Gonzalito-Sierra Pailemán (c), and Sierra Grande (d) areas. Fig. 1b depicts location of map of Fig. 2. Fig. 1b–d shows detrital zircon sample locations and maximum depositional ages from this contribution and other authors.

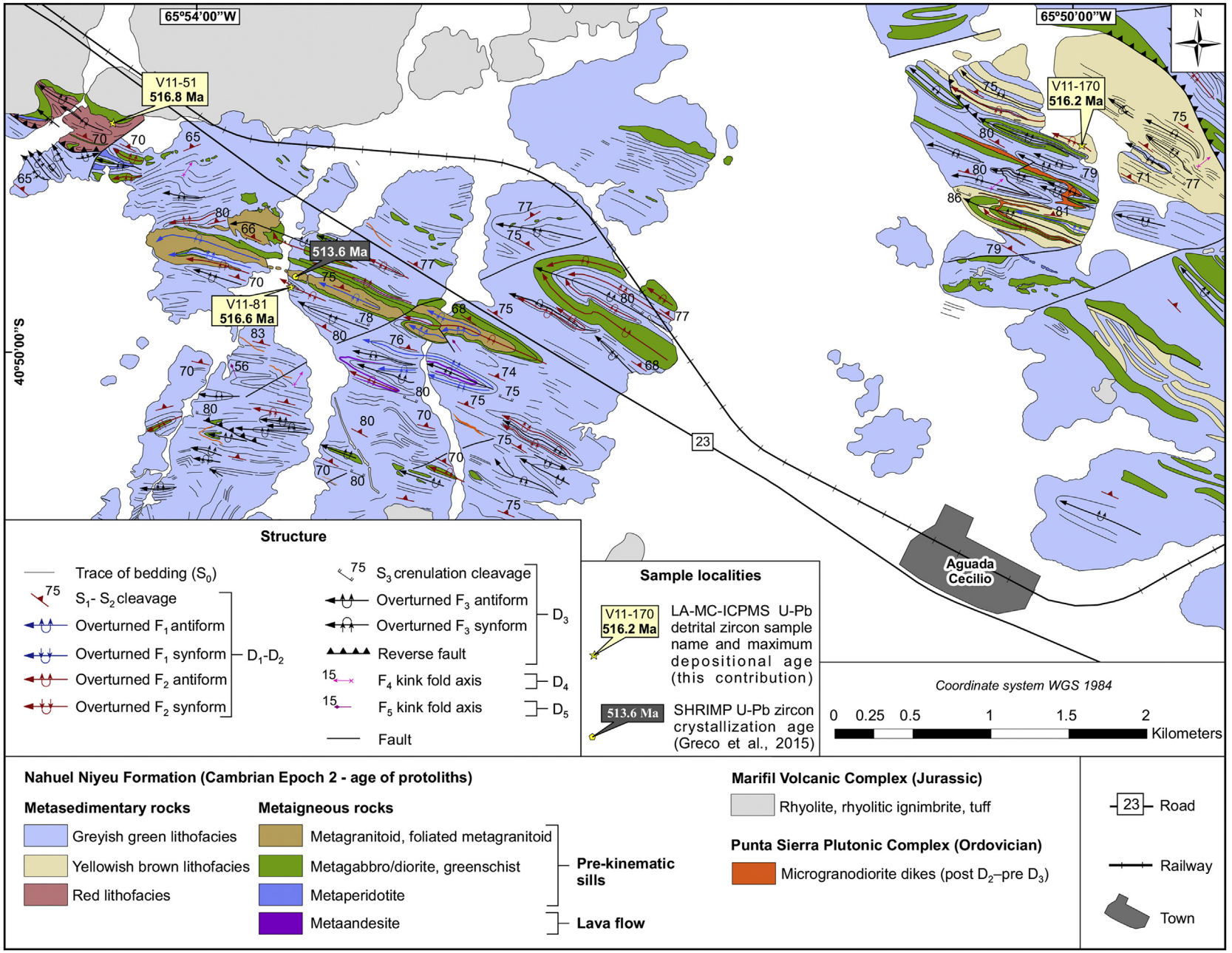

Fig. 2. Geological map of the surroundings of Aguada Cecilio with sample localities. Mapping of the structure and the igneous bodies is based on Greco et al. (2015). For location of map see Fig. 1b. D_1, D_2, D_3, D_4 and D_5 correspond to the deformation structures depicted in Fig. 4.

Ma depositional ages for the marble protoliths (Varela et al., 2014). A NNW–SSE to NW–SE trending fabric related to two successive deformation stages associated with amphibolite facies regional metamorphism of Early Ordovician age (metamorphic zircon rims dated at 472 Ma in Pankhurst et al., 2006) characterizes the complex (Giacosa, 1987, 1997; González et al., 2008a). Metamorphic climax was reached during the second deformation stage and accompanied by the intrusion of the syntectonic leucogranites (González et al., 2008a). The protolith of the granodioritic orthogneiss was intruded between the two deformation stages (intertectonic) (González et al., 2008a). A SHRIMP U–Pb zircon age of 492 Ma constrains the timing of magmatic crystallization of the granodioritic orthogneiss (Varela et al., 2011a). The brittle-ductile El Jagüelito shear zone juxtaposes the Mina Gonzalito Complex against the Peñas Blancas Pluton belonging to the Punta Sierra Plutonic Complex (Fig. 1c; Ramos, 1975; Ramos and Cortés, 1984; Giacosa, 1997; García et al., 2014a). The El Jagüelito shear zone as well as the Peñas Blancas shear zone represent the Permian tectonism in the Mina Gonzalito–Sierra Pailemán area (Giacosa, 2001; von Gosen, 2002).

The El Jagüelito Formation (Giacosa, 1987) crops out in the Mina Gonzalito-Sierra Pailemán and Sierra Grande areas, but it is well exposed in the latter (Fig. 1c and d). It consists of slates, phyllites, metagreywackes, lithic metaarenites, and minor polymictic metaconglomerates, intercalations of metatuffs, metaignimbrites, metaandedesitic and metarhyolitic lava flows, and metarhyolitic dikes and domes (de Alba, 1964; Giacosa, 1987; Giacosa and Paredes, 2001; González et al., 2002, 2008b, 2011b, 2011c, 2013; Dalla Salda et al., 2003a; González, et al., 2014a). SHRIMP and LA–ICPMS U-Pb detrital zircon data constrain maximum depositional ages of siliciclastic protoliths between 535 Ma (sample SGR-018, Pankhurst et al., 2006) and 523 Ma (sample AB-282, Naipauer et al., 2010) (Fig. 1d). Archeocyath fossils in limestone blocks of a metaconglomerate indicate a Cambrian Epoch 2 (Atdabanian–Botomian, between 521 and ~513 Ma) maximum depositional age for the metaconglomerate protolith (González et al., 2011b). NNW–SSE to NNE–SSW-trending fabric associated with regional greenschist-facies metamorphism characterizes the El Jagüelito Formation (Giacosa and Paredes, 2001; von Gosen, 2002; González et al., 2008b, 2011b, 2011c; González, et al., 2014a). Early Ordovician granitoids belonging to the Punta Sierra Complex with conventional and SHRIMP U–Pb zircon ages between 476 and 462 Ma (Varela et al., 1998, 2008; Pankhurst et al., 2006; González et al., 2008c) intrude the El Jagüelito Formation after the first tectonometamorphic event (von Gosen, 2002; González et al., 2008b).

The Las Grutas igneous–metamorphic complex occurs south of Las Grutas in small and scattered outcrops (Fig. 1) and consists of paragneisses, schists, amphibolites, orthogneisses and granites (e.g. Piedras Coloradas granite) (Sato et al., 1998). An Rb–Sr errorchrone age of 409 Ma for the Piedras Coloradas granite (Varela et al., 1997) is the only geochronological data available of this complex.

Silurian-Devonian sandstones of the Sierra Grande Formation represent the Paleozoic sedimentary cover in Nahuel Niyeu–Aguada Cecilio and Sierra Grande areas. The sandstones unconformably cover the Nahuel Niyeu and El Jagüelito formations and are affected by the Permian tectonism (Núñez et al., 1975; Zanettini, 1981; Caminos, 1983, 2001; Chernicoff and Caminos, 1996a; Busteros et al., 1998; von Gosen, 2002, 2003).

Granitoid plutons belonging to the Navarrete and Pailemán plutonic complexes and representing a widespread Permian magmatic event intrude all the previously mentioned units (Giacosa, 1997; Caminos, 2001; Pankhurst et al., 2006; Varela et al., 2008; López de Luchi et al., 2008; Gozalvez, 2009a; García et al., 2014b; Martínez Dopico et al., 2016).

After the Permian tectonic and magmatic events, Triassic to Jurassic magmatic and sedimentary units develop in wide areas of the eastern North Patagonian Massif (Malvicini and Llambías, 1974; Cortés, 1981; Caminos, 1983, 2001; Pankhurst et al., 1993; Pankhurst and Rapela, 1995; Aragón et al., 1996; Pankhurst et al., 1998; López de Luchi et al., 2008; Márquez et al., 2011; González, et al., 2014b; González et al., 2016, 2017).

Late Cretaceous to Cenozoic sedimentary and volcanic rocks cover all previously mentioned geological units (Busteros et al., 1998; Martínez et al., 2001; Caminos, 2001).

3. Geology of the Nahuel Niyeu Formation in the Aguada Cecilio area

3.1. Lithology

In the Aguada Cecilio area (Fig. 2), the metasedimentary rocks of the Nahuel Niyeu Formation consist mainly of alternating metagreywackes and phyllites, and minor metaarenites (Greco et al., 2015). They also include intercalations of metaigneous rocks (Giacosa, 1999; Greco et al., 2015). Both the metasedimentary and metaigneous rocks develop an S_1–S_2 cleavage, which is the dominant and penetrative foliation of the Nahuel Niyeu Formation (Greco et al., 2015; see synthesis of the Section 3.2).

3.1.1. Metasedimentary rocks

On the basis of lithology and color, the metasedimentary rocks are grouped into three informal lithofacies that allow rapid identification and mapping in the field: greyish green, yellowish brown and red lithofacies (Figs. 2 and 3a–f). Contacts between different metasedimentary rocks define the relict bedding (S_0) of the metasedimentary succession (Figs. 2 and 3a, e). Regional metamorphism and deformation have obliterated and obscured sedimentary structures that may indicate polarity of beds.

The greyish green lithofacies is the most typical facies in Aguada Cecilio area (Fig. 2). It consists of alternating massive metagreywackes, foliated metagreywackes, laminated metagreywackes and greyish green phyllites (Fig. 3a, b and c).

The yellowish brown lithofacies (Fig. 3d) consists of laminated metagreywackes and minor intercalations of greyish green phyllites, the latter similar to those of the greyish lithofacies. The rocks of the yellowish brown lithofacies alternate with those of the greyish green lithofacies. An NNE-dipping reverse fault juxtaposes these lithofacies in the northeastern outcrops (Fig. 2).

The red lithofacies consist of massive metagreywackes and foliated metagreywackes, and minor metaarenites and red phyllites (Fig. 3e and f). Additionally, this metasedimentary succession has metatuff levels of up to 1 cm thick (Fig. 3f). The red lithofacies crops out in a small area where a high-angle reverse fault juxtaposes it against the greyish green lithofacies (Fig. 2).

3.1.2. Metaigneous rocks

Metagabbro/diorites, and minor metaperidotites and metagranitoids are interpreted as a pre-kinematic sill swarm, whereas metaandesites as a subaqueous lava flow (Fig. 2; Greco et al., 2015). The sill swarm comprises simple and composite intrusive bodies, according to the composition (Greco et al., 2015), and intrude the three lithofacies. The lava flow is interbedded in the greyish green lithofacies. Border zones of the sills are transformed into greenschists or foliated metagranitoids according to their composition, and develop the S_1–S_2 foliation (see details in Greco et al. (2015)).

A SHRIMP U–Pb zircon age of 513.6 ± 3.3 Ma from a composite sill is assigned to the crystallization age of the entire sill swarm on the basis of a spatial, temporal and genetic connection between the intrusive rocks (Fig. 2; Greco et al., 2015). Geochemical characteristics of the sills indicate subduction related tholeiitic magmatism

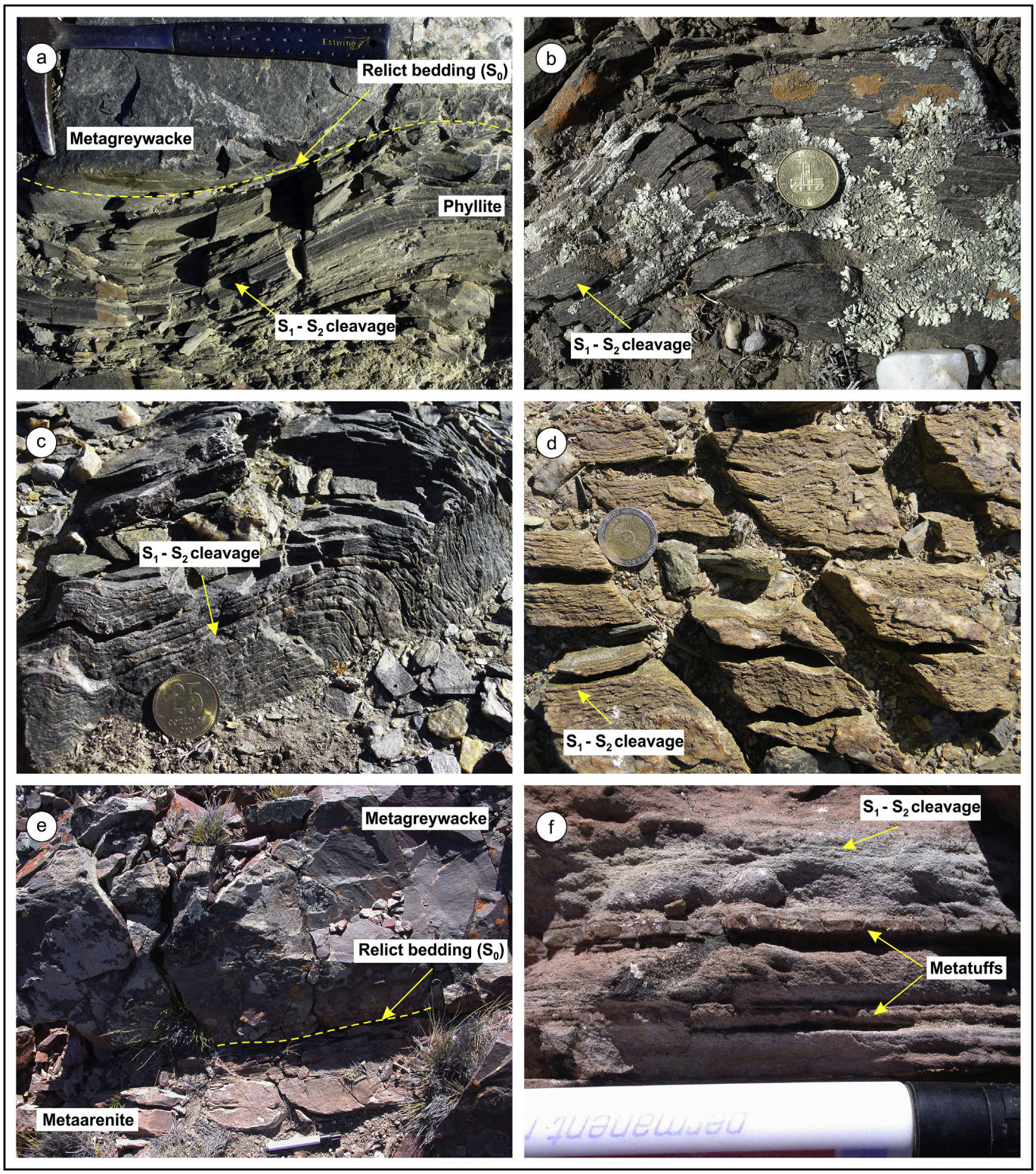

Fig. 3. Outcrop features of the metasedimentary rocks from the Nahuel Niyeu Formation in the Aguada Cecilio area. Note the characteristic color of each lithofacies. (a) Relict bedding (S_0) defined by the contact between a massive metagreywacke and a phyllite of the greyish green lithofacies. The phyllite exhibits an S_1–S_2 cleavage. (b) Foliated metagreywacke of the greyish green lithofacies displaying S_1–S_2 cleavage affected by a F_4 kink fold. (c) Laminated metagreywacke of the greyish green lithofacies showing S_1–S_2 cleavage. F_3 folds affect the S_1–S_2 cleavage. (d) Laminated metagreywacke of the yellowish brown lithofacies. F_4 kink folds affect S_1–S_2 cleavage. (e) Massive metagreywacke in contact with a metaarenite, both belonging to the red lithofacies. The contact defines the relict bedding (S_0). (f) Thin levels of metatuffs intercalated with metaarenites of the red lithofacies. (For interpretation of the references to colour in this figure legend, the reader is referred to the web version of this article.)

and involvement of continental crust (Greco et al., 2015).

3.2. Deformation stages and associated regional metamorphism

Five deformation stages (D_1 to D_5), which produced D_1, D_2, D_3, D_4 and D_5 deformation structures, and two regional metamorphic events (M_1 and M_2) affected both the metasedimentary and metaigneous rocks in the Aguada Cecilio area (a detailed description of the structure, microfabrics and associated metamorphism is in Greco et al., 2015). Fig. 4 summarizes these processes.

4. Petrography of the metasandstones

We performed petrographic studies of the metasandstones from the Nahuel Niyeu Formation in Aguada Cecilio area, putting emphasis on the description and analysis of relict sedimentary features preserved in these rocks, such as detrital grains and recrystallized fine matrix. The results, together with our new detrital zircon data (Section 5) and previous geochronological, petrographical and geochemical data, are discussed in sections 6.2 and 6.3 in order to provide significant information about the siliciclastic protoliths and their source rocks. We determined sorting and roundness of detrital grains with visual comparators (Pettijohn et al., 1987; Jerram, 2001). It was not possible to perform quantitative modal analyses because of the difficulty in distinguishing small relict detritus from the recrystallized matrix.

The metasandstones of the three lithofacies preserve relict, coarse silt- to sand-sized detrital grains surrounded by a recrystallized, fine relict matrix (Figs. 5a–f and 6a–f). They exhibits a similar, relict detrital composition containing abundant detrital grains of quartz, plagioclase and alkali feldspar, and minor muscovite, apatite, epidote, rutile, titanite and zircon (Figs. 5a–f and 6a–f). Variable proportions of lithic fragments also are contained in the relict detrital composition of the metasandstones. The lithic fragments are particularly abundant in the massive metagreywackes that are the rocks preserving coarser-grained detrital grains, whereas in the foliated and laminated metagreywackes and metaarenites they are a minor component. Some quartz grains preserve part of a hexagonal/bipyramidal shape with straight sides and embayments, features that suggest a volcanic origin (Figs. 5a, b, d and 6c). In addition, some sieved plagioclase grains occur indicating the same origin (Figs. 5b, f and 6c, d), whereas alkali feldspar grains with perthitic and granophyric textures suggests a plutonic origin. Lithic fragments are igneous and metamorphic. The igneous fragments are acidic volcanic rocks with fenocrysts of quartz in a felsitic groundmass, acidic volcanic rocks with fenocrysts of quartz in a recrystallized and foliated groundmass, felsitic groundmass, and microgranites (Figs. 5a–d and 6b, d, f). The metamorphic fragments are phyllites (Fig. 5a), polycrystalline quartz with granoblastic texture (Fig. 5c and d), and polycrystalline quartz with sutured internal boundaries (Fig. 6b), the latter two probably derived from schists and gneisses.

The relict detrital grains of the metasandstones of the three lithofacies are poorly sorted and most of them preserve their angular to subrounded original shape (Figs. 5a–e and 6b–e). Numerous detrital grains of quartz, plagioclase and alkali feldspars are commonly flattened parallel to the S_1–S_2 cleavage in the foliated and laminated metagreywackes and metaarenites (Figs. 5e, f and 6a, e, f). Microstructures evidencing processes of intracrystalline deformation and partial recrystallization are present in the relict detrital grains of quartz, plagioclase and alkali feldspar (e.g. undulose extinction, deformation bands, subgrains, and new grains in their boundaries; Figs. 5a–f and 6a–f). These microstructures are associated with regional metamorphism and deformation that affected the Nahuel Niyeu Formation (Greco et al., 2015).

The recrystallized matrix is abundant in the metagreywackes and scarce in metaarenites, and is composed of metamorphic minerals forming comparable mineral parageneses in the

Geologic time	Deformation stages and structure		Metamorphism
late Permian or younger?	D_5	NNW–SSE-trending F_5 kink folds	
	D_4	NE–SW-trending F_4 kink folds	
late Permian	D_3	Tight to isoclinal WNW–ESE-trending F_3 folds and high-angle reverse faults; S_3 axial plane crenulation cleavage; F_3 fold axes are parallel to F_1 and F_2 axes; tectonic transport to the SSW	M_2 regional metamorphism in the chlorite zone of the greenschist facies
end of the Cambrian Epoch 2 to Early Ordovician	D_2	Isoclinal and similar WNW–ESE-trending F_2 folds; F_2 folds are coaxial with F_1 folds; penetrative S_2 axial plane cleavage; the S_1 and S_2 cleavages are subparallel in the limbs of F_1 and F_2 and form the S_1–S_2 cleavage (dominant and penetrative foliation)	M_1 regional metamorphism in the biotite zone of the greenchist facies; metamorphic climax reached during D_2
	D_1	Isoclinal and similar WNW–ESE-trending F_1 folds; penetrative S_1 axial plane cleavage	

Fig. 4. Synthesis of deformation stages and associated regional metamorphism of the Nahuel Niyeu Formation in the Aguada Cecilio area (simplified and schematic chart). Modified after Greco et al. (2015).

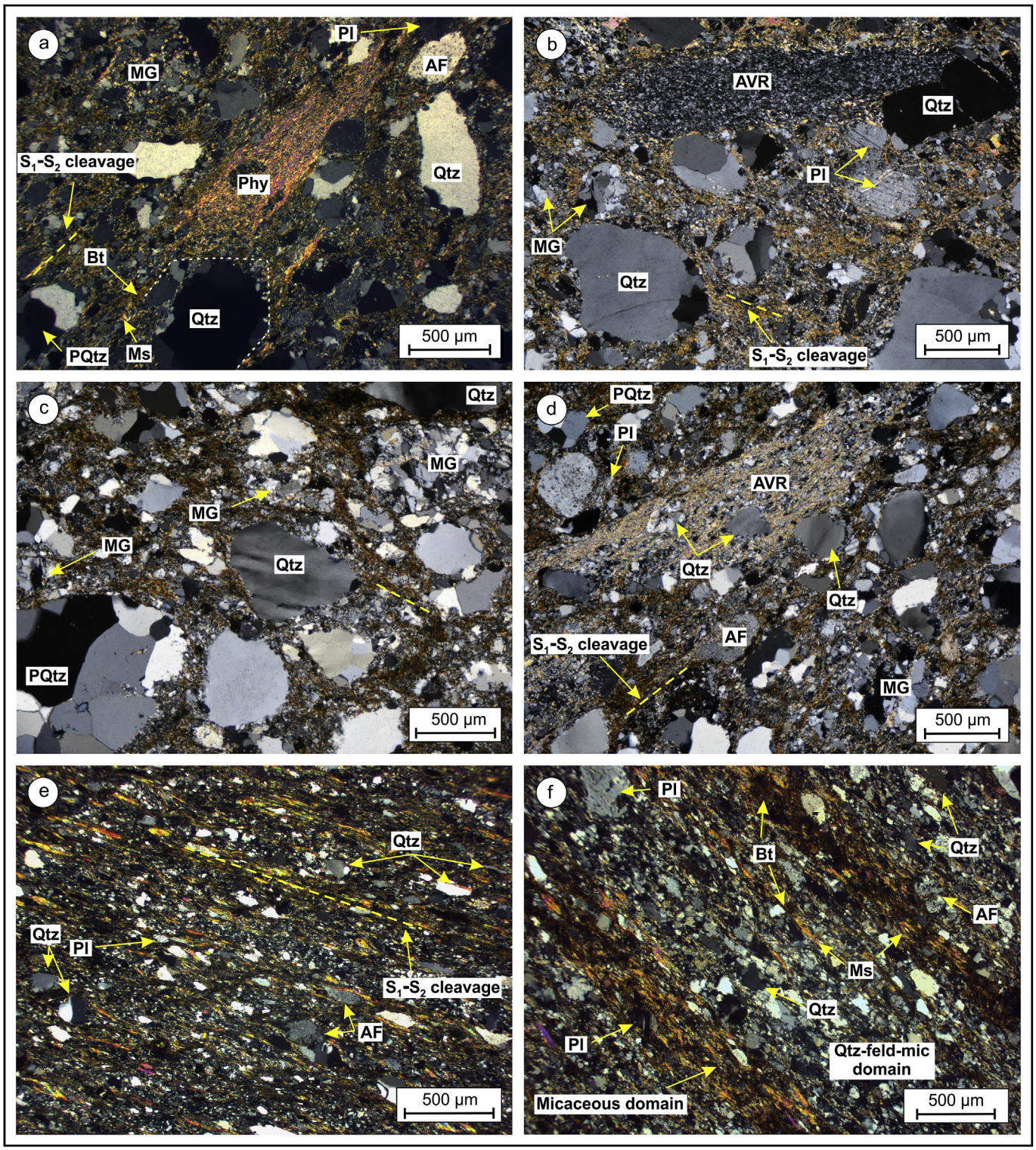

Fig. 5. Photomicrographs of the greyish green lithofacies metagreywackes. Crossed nicols in all photomicrographs. Detrital grains: Qtz (quartz), Pl (plagioclase), AF (alkali feldspar), PQtz (polycrystalline quartz); MG (microgranite), AVR (acidic volcanic rock) and Phy (phyllite). Metamorphic minerals: Bt (biotite) and Ms (muscovite). (a), (b) (c) and (d) Massive metagreywacke with angular to subrounded, relict detrital grains of quartz, plagioclase, alkali feldspar, and metamorphic (coarse-grained polycrystalline quartz with granoblastic texture and phyllite) and igneous fragments (microgranite and acidic volcanic rock). A recrystallized, fine relict matrix surrounds the detritus and contains biotite and muscovite of the metamorphic mineral paragenesis forming an S_1–S_2 rough cleavage (dotted line). Acidic volcanic rocks in (b) and (d) exhibit fenocrysts of quartz (quartz that appears black in the upper right corner) in a felsitic groundmass and fenocrysts of quartz in a recrystallized and foliated groundmass, respectively. The quartz grain indicated in (a) and that out of the clast of the acidic volcanic rock in (d) preserve part of a hexagonal shape with straight sides (grey dotted line in a). The plagioclase in (b) is sieved. (a), (b), (c) and (d) are photomicrographs of the sample V11-81. (e) Foliated metagreywacke angular to subrounded relict detrital grains and an S_1–S_2 continuous cleavage. Some quartz and alkali feldspar detrital grains are flattened according to the S_1–S_2 cleavage. (f) Laminated metagreywacke with S_1–S_2 disjunctive cleavage and relict detrital grains of quartz, plagioclase and alkali feldspar. Some of these grains are flattened according to the S_1–S_2 cleavage. The plagioclase of the upper left corner is sieved. Most detrital grains of quartz in (a–f) exhibit undulose extinction, deformation bands, and subgrains and new grains in their boundaries. (For interpretation of the references to colour in this figure legend, the reader is referred to the web version of this article.)

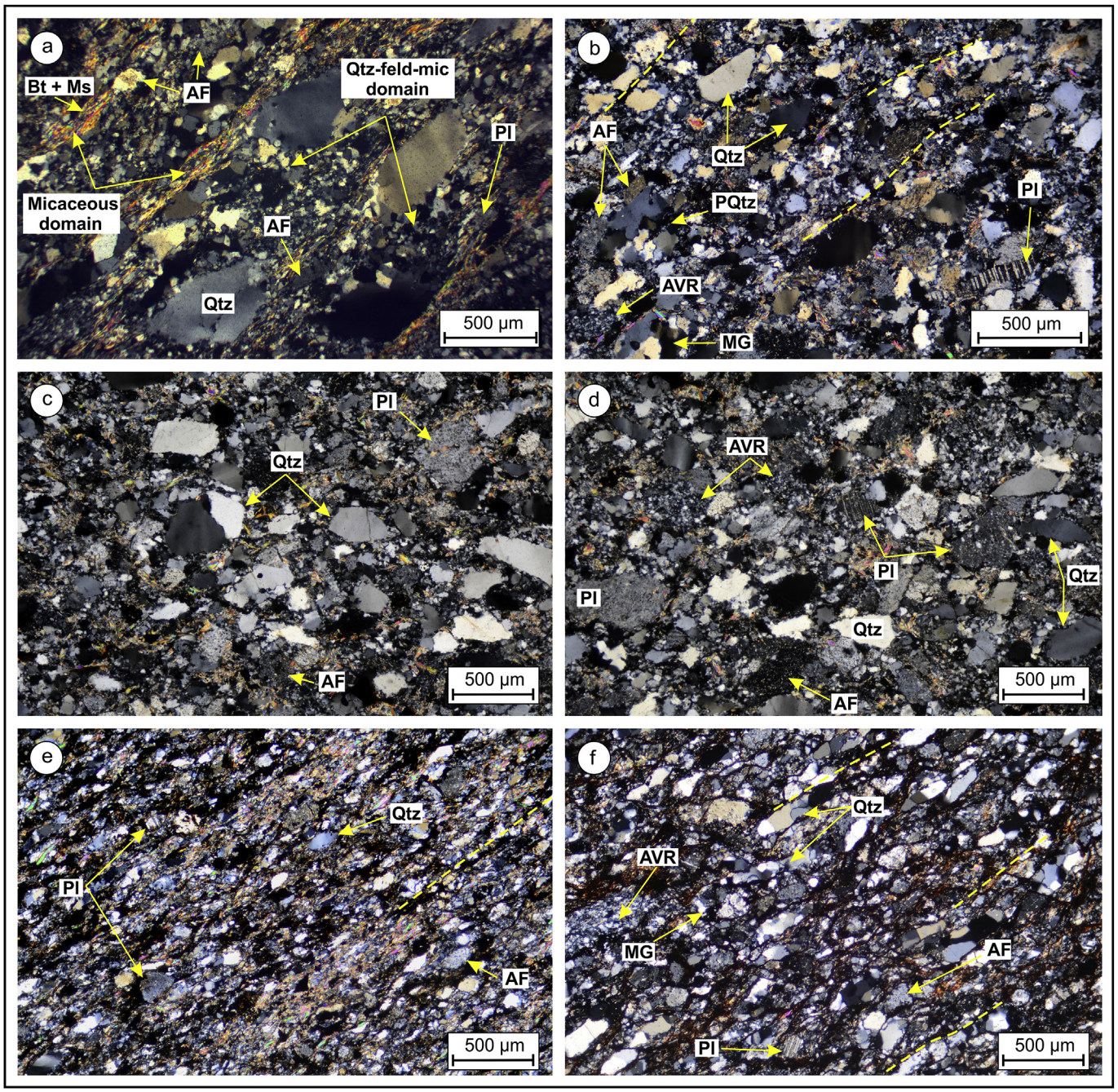

Fig. 6. Photomicrographs of metasandstones from the yellowish brown and red lithofacies. Crossed nicols in all photomicrographs. Abbreviations of detrital grains and metamorphic minerals are the same as in Fig. 4. (a) Laminated metragreywacke from the yellowish brown lithofacies. It is a photomicrograph of the sample V11-170. Alternating micaceous and quartz-feldspathic-micaceos domains form an S_1–S_2 disjunctive cleavage. Quartz detrital grains present undulose extinction, deformation bands, and subgrains and new grains in the boundaries which are transitional with the recrystallized matrix. (b), (c) and (d) Massive metagreywacke from the red lithofacies. These are photomicrograph of the sample V11-51. The metagreywacke preserves angular to subrounded, relict detrital grains of quartz, alkali feldspar, plagioclase, polycrystalline quartz with sutured internal boundaries, microgranite and felsitic groundmass fragments (acidic volcanic rocks). Dotted line in (b) indicates the S_1–S_2 rough cleavage of the rock. Quartz grains indicated in (c) preserves their hexagonal shape with straight sides. The plagioclase grains indicated in (c) and (d) are sieved. e) Foliated metagreywacke of the red lithofacies. It present a continuous S_1–S_2 cleavage (dotted line). Relict detrital grains preserve their angular to subrounded original shape, however some of them are flattened according to the cleavage. (f) Metaarenite of the red lithofacies. Flattened detrital grains of quartz, plagioclase, alkali feldspar, microgranite and felsitic groundmass fragments occur. Dotted lines mark the continuous S_1–S_2 cleavage. (For interpretation of the references to colour in this figure legend, the reader is referred to the web version of this article.)

metasandstones of all lithofacies. Biotite + muscovite + chlorite + quartz + albite are metamorphic minerals present in all parageneses suggesting greenschist facies metamorphism. The metamorphic phyllosilicates define the S_1–S_2 cleavage, which is rough in massive metagreywackes (Figs. 5a–d and 6b–d), continuous in foliated metagreywackes and metaarenites (Figs. 5e and 6e, f) and disjunctive in laminated metagreywackes (Figs. 5f and 6a). The S_1–S_2 disjunctive cleavage that is defined by alternating quartz-feldspathic-micaceous and micaceous domains might reflect a relict fine intercalation of pelitic and psamitic protoliths (S_0). The abundance of metamorphic biotite and chlorite gives the characteristic color to the greyish green lithofacies. Compared to the

Table 1
Morphological classes of detrital zircons from the analyzed metasedimentary rocks.

	Class 1	Class 2	Class 3	Class 4	Class 5	Class 6	Class 7
Shape	pr[a]	pr[a]	st[b]	st[b]	ov[c]	eq[d]	eq[d]
Aspect ratio	≥2	≥2	<2–>1.2	<2–>1.2	≤1.9–≥1.3	≤1.2–1	≤1.2–1
Degree of roundness	pur-vpr[e]	sr[f]	pur-vpr[e]	sr[f]	rd[g]	sr[f]	rd[g]

[a] Prismatic.
[b] Stubby.
[c] Ovoid.
[d] Equant.
[e] Practically unrounded to very poorly rounded.
[f] Subrounded.
[g] Rounded.

greyish green lithofacies, metamorphic biotite and chlorite are scarcer in the yellowish lithofacies, which explains the color difference. Particularly, the red lithofacies exhibits abundant metamorphic opaque minerals and oxides in their parageneses, which provide the red color to this lithofacies.

5. Detrital zircon geochronology

We determined LA–MC–ICPMS U–Pb ages and characteristics of detrital zircon grains in three samples of metagreywacke from the Nahuel Niyeu Formation in Aguada Cecilio area, each one from a different lithofacies (samples V11-81, V11-170 and V11-51 in Fig. 2; Figs. 5a, b, c, d, 6a, b, c and d). Appendix A contains location and description of the samples, LA–MC–ICPMS U–Pb analytical procedure, method of zircon grain characterization, and method for determining maximum depositional ages.

5.1. Results

We randomly analyzed by LA–MC–ICPMS U–Pb method ninety one, eighty five and ninety detrital zircons from the samples V11-81, V11-170 and V11-51, respectively. This section first presents the morphological characteristics of the analyzed detrital zircon grains and then the LA–MC–ICPMS U–Pb results.

5.1.1. Morphology of detrital zircon grains

The analyzed zircon grains from the three samples show differences in morphological features such as shape and degree of roundness. They have prismatic, stubby, ovoid and equant shapes with aspect ratios ranging from 3.1 to 1. The degree of roundness is highly variable, but we classify it in three groups: 1- practically unrounded to very poorly rounded, 2- subrounded and 3- rounded. This classification is a simplification of the ten classes of roundness of zircon grains defined by Gärtner et al. (2013). The grains of the first group show edges and angles well defined, although some of the edges and angles can be slightly rounded. Subrounded grains display almost all edges and angles rounded, but preserve some of them well defined. Rounded grains have all edges and angles well rounded.

The global analysis of the morphological features from the detrital zircons of each sample, allowed us to classify them into seven morphological classes, which are summarized in the Table 1.

Table 2 depicts the morphological classes present in the samples, including length, aspect ratio and number of grains. The sample V11-81 shows zircon grains from the classes 2, 4, and 6 (46 grains) and from the classes 5 and 7 (29 grains). The sample V11-170 exhibits a large number of zircons from the classes 2, 4, and 6 (57 grains) and less from the classes 1 and 3 (9 grains), and 5 and 7 (10 grains). The sample V11-51 has a large number of zircons from the classes 1 and 3 (40 grains) and less from the classes 2, 4 and 6 (32 grains), and 5 and 7 (13 grains).

5.1.2. LA–MC–ICPMS U–Pb results

Tables A1, A2 and A3 of the Appendix A summarize the U–Pb results of the samples, including site of analysis (spot), morphological characteristics and classes, internal structure, and inferred origin of the zircon grains. The analyzed detrital grains show similar U–Pb ages in the three samples, which range from Cambrian to Archean. From this similarity, we group the analyzed detrital zircons into six populations (P1 to P6) according to their U–Pb ages. The six populations are represented in the three samples, but with slight differences in age and variable proportion. P1 and P6 correspond to the youngest and oldest population, respectively. Figures A1, A2 and A3 of the Appendix A illustrate the CL images of zircon populations from each sample. Tables 3, 4 and 5 contain detailed characteristics of the zircon populations.

Table 2
Physical properties of detrital zircons from the analyzed samples.

	Class 1	Class 2	Class 3	Class 4	Class 5	Class 6	Class 7
Sample V11-81 - greyish green lithofacies							
Lenght	–	193–130	–	170–111	159–94	152–99	118–83
Aspect ratio	–	2.7–2	–	1.9–1.3	1.8–1.3	1.2–1	1.2–1
n	–	17	–	23	18	6	11
Sample V11-170 - yellowish brown lithofacies							
Lenght	187–150	191–137	164–106	164–96	138–108	117–93	137–90
Aspect ratio	2.5–2.3	2.7–2	1.9–1.4	1.9–1.3	1.9–1.4	1.2–1	1.1–1
n	3	17	6	31	7	9	3
Sample V11-51 - red lithofacies							
Lenght	203–112	187–124	163–88	168–105	152–94	129–89	130–93
Aspect ratio	3.1–2	2.9–2	1.8–1.3	1.9–1.3	1.7–1.3	1.2–1	1.2–1.1
n	26	11	14	16	8	5	5

n = number of zircon grains. Lenght = maximum and minimum values (μm).

Table 3
Detailed characteristics of the zircon populations from the sample V11-81.

	P1	P2	P3	P4	P5	P6
Age max–min (Ma)	515–558	561–634	663–925	961–1239	1863–2001	2554
Major probability (Ma)	558	585	778	1020	1987	2554
Minor probability (Ma)	516, 536, 542	615	663, 710, 734, 758, 833, 860, 890, 925	963, 1060, 1160, 1174, 1239	1863	
n	13	25	12	21	3	1
% of the total pattern	17	33	16	28	4	1
Class 1 (n)	0	0	0	0	0	0
Class 2 (n)	1	3	4	7	1	1
Class 3 (n)	0	0	0	0	0	0
Class 4 (n)	7	5	3	7	1	0
Class 5 (n)	3	9	2	4	0	0
Class 6 (n)	2	2	1	1	0	0
Class 7 (n)	0	6	2	2	1	0
Magmatic zircons (n)	8	11	10	12	2	1
Metamorphic zircons (n)	5	14	2	9	1	0
Total magmatic zircons (n)	44 (59%)					
Total metamorphic zircons (n)	31 (41%)					

n = number of zircon grains.

Table 4
Detailed characteristics of the zircon populations from the sample V11-170.

	P1	P2	P3	P4	P5	P6	Isolated age
Age max–min (Ma)	511–556	563–650	673–833	964–1054	1839–2028	2634	1418
Major probability (Ma)	521	610	705	985	1839, 1876, 1967, 2028	2634	1418
Minor probability (Ma)	533, 553	561, 583	673, 744, 770, 810, 833	1010, 1050, 1054			
n	44	10	10	6	4	1	1
% of the total pattern	58	13	13	8	5	1.5	1.5
Class 1 (n)	3	0	0	0	0	0	0
Class 2 (n)	11	2	3	0	0	1	0
Class 3 (n)	6	0	0	0	0	0	0
Class 4 (n)	20	3	5	2	1	0	0
Class 5 (n)	0	1	2	2	2	0	0
Class 6 (n)	4	4	0	0	0	0	1
Class 7 (n)	0	0	0	2	1	0	0
Magmatic zircons (n)	43	8	7	4	2	0	1
Metamorphic zircons (n)	1	2	3	2	2	1	0
Total magmatic zircons (n)	65 (85%)						
Total metamorphic zircons (n)	11 (14%)						

n = number of zircon grains.

Table 5
Detailed characteristics of the zircon populations from the sample V11-51.

	P1	P2	P3	P4	P5	P6
Age max–min (Ma)	512–553	569–640	662–920	963–1168	1869–1981	2597–2722
Major probability (Ma)	524	602	688	1030	1869, 1981	2597, 2649, 2720
Minor probability (Ma)	552	572, 627, 640	662, 768, 868, 920	976, 1014, 1066, 1145, 1168		
n	44	11	7	17	2	4
% of the total pattern	52	13	8	20	2	5
Class 1 (n)	26	0	0	0	0	0
Class 2 (n)	0	5	0	6	0	0
Class 3 (n)	13	0	1	0	0	0
Class 4 (n)	3	4	3	5	0	1
Class 5 (n)	0	1	0	5	1	1
Class 6 (n)	2	1	1	0	1	0
Class 7 (n)	0	0	2	1	0	2
Magmatic zircons (n)	43	9	4	14	1	3
Metamorphic zircons (n)	1	2	3	3	1	1
Total magmatic zircons (n)	74 (87%)					
Total metamorphic zircons (n)	11 (13%)					

n = number of zircon grains.

Concordia diagrams (Fig. A4 of the Appendix A), frequency histograms, relative probability plots, and weighted-mean age and Unmix routine plots (Fig. 7a, b and c) show the filtered U–Pb data.

Sample V11-81 (greyish green lithofacies): The ninety one analyzed zircons are concordant (<10% of discordance), however, we discarded sixteen of them because of high (>6%) ^{206}Pb of common origin. Without a prominent youngest probability peak like in the case of the remaining samples, the pattern of detrital zircon ages is characterized by abundant Neoproterozoic and Mesoproterozoic ages, with minor Cambrian, Paleoproterozoic and Archean ages. In detail, the pattern comprises (Fig. 7a and Fig. A1 and Table 3): (1) a P1 population (17% of the pattern) of igneous

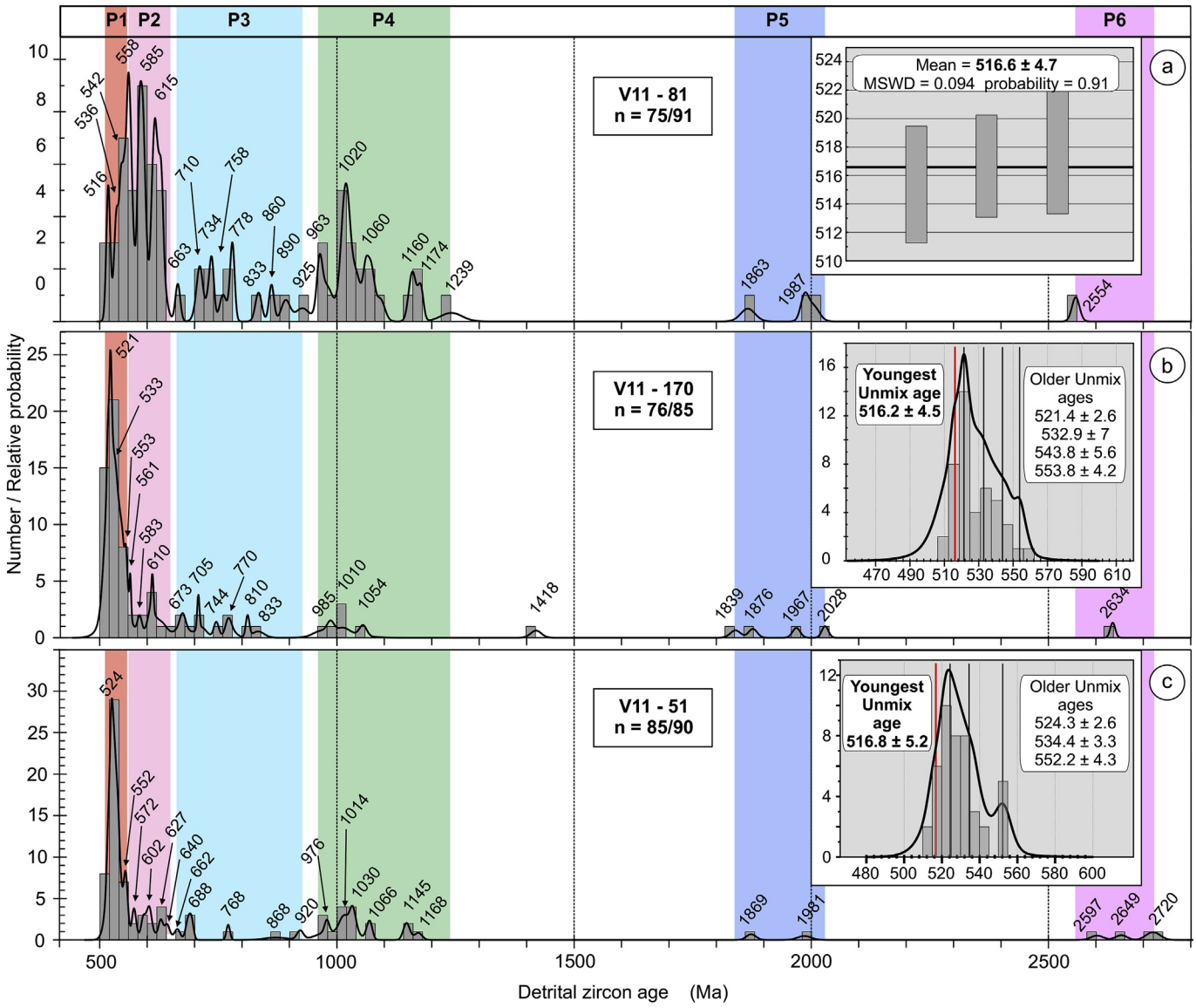

Fig. 7. Relative probability plots (curves) and frequency histograms (grey bars) of detrital zircon ages, and maximum depositional ages from the samples V11-81 (a), V11-170 (b) and V11-51 (c). n = number of filtered individual grains (grains with <6% of ^{206}Pb of common origin/total analyzed grains). Numbers over the curves indicate ages of probability peaks. Color bars represent the ages of the populations of zircon grains (P1, 511–558 Ma; P2, 561–650 Ma; P3, 662–925 Ma; P4, 961–1239 Ma; P5, 1839–2028 Ma; P6, 2554–2722 Ma). Age limits of the color bars correspond to the maximum and minimum age of each population considering all samples. In (a) is represented the weighted-mean age of the youngest discrete cluster of three grain ages (maximum depositional age), all with an igneous origin. In (b) and (c) are represented the Unmix routine applied to the youngest components of the distribution of detrital zircon ages of each sample (P1 grains). These graphics show the youngest (red vertical lines) and older (black vertical lines) Unmix ages in relative probability plots (curves) and frequency histograms (grey bars). The youngest Unmix ages represent the maximum depositional ages. Uncertainties for weighted-mean and Unmix ages are at 2σ. Box heights in the weighted-mean age are at 1σ. (For interpretation of the references to colour in this figure legend, the reader is referred to the web version of this article.)

and minor metamorphic grains with ages in the range of 515 Ma to 558 Ma belonging to the morphological classes 2, 4, 5, and 6 and defining the youngest and the major probability peaks of the sample at 516 and 558 Ma; (2) a P2 population (33% of the pattern) of metamorphic and igneous zircon grains from the morphological classes 2, 4, 5, 6 and 7, with ages from 561 Ma to 634 Ma and a major peak at 585 Ma; (3) a P3 population (16% of the pattern) of mainly igneous grains from the morphological classes 2, 4, 5, 6 and 7, with ages between 663 and 925 Ma and a major peak at 778 Ma; (4) a P4 population (28% of the pattern) of igneous and metamorphic grains from the morphological classes 2, 4, 5, 6 and 7, with ages between 961 Ma and 1239 Ma and a major probability peak at 1020 Ma; (5) three Paleopropterozoic ages and an Archean age complete the pattern and they correspond to the P5 and P6 populations, respectively. The youngest discrete cluster of three grain ages (all grains have igneous origin) yielded a weighted-mean age of 516.6 ± 4.7 Ma (MSWD = 0.094), which constrains the deposition of the siliciclastic protolith of this metagreywacke of the greyish green lithofacies to the Cambrian Epoch 2 or younger (Fig. 7a). This age is similar to the youngest probability peak of the sample at 516 Ma, because this peak exclusively represents the youngest discrete cluster of three grains.

Sample V11-170 (yellowish brown lithofacies). The eighty five executed zircons are concordant (<10% of discordance), but we rejected nine of them because of high (>6%) ^{206}Pb of common origin. The pattern of detrital zircon ages is characterized by abundant Cambrian and latest Neoproterozoic ages, with minor Neoproterozoic, Mesoproterozoic, Paleoproterozoic and Archean

ages. The pattern comprises (Fig. 7b, Fig. A2 and Table 4): (1) a P1 population (58% of the pattern) virtually all composed of igneous zircons from morphological classes 1, 2, 3, 4 and 6, in the range of 511 Ma to 556 Ma and with the youngest and major probability peak of the sample at 521 Ma; (2) P2 and P3 populations of mainly igneous zircons from the morphological classes 2, 4, 5 and 6, and with ages between 563 Ma to 650 Ma (13% of the pattern and a major probability peak at 610 Ma) and 673 Ma to 833 Ma (13% of the pattern and a major probability peak at 705 Ma), respectively; (3) two populations of igneous and metamorphic zircons from the morphological classes 4, 5 and 7 that range from 964 to 1054 Ma (P4, 8% of the pattern, major peak at 985 Ma) and 1839–2028 Ma (P5, 5% of the pattern); (4) two isolated ages at 1418 and 2634 Ma, the latter corresponds to the P6 population. The youngest Unmix age of 516.2 ± 4.5 Ma (calculed from the P1 grains -youngest components-) suggests a Cambrian Epoch 2 or younger depositional age for the protolith of this metagreywacke from yellowish brown lithofacies (Fig. 7b). This age is younger than the youngest probability peak of the sample at 521 Ma, because this peak represents both the youngest cluster of grain ages (Unmix age = 516.2 ± 4.5) and the contiguous group with slightly older ages.

Sample V11-51 (red lithofacies): The ninety analyzed zircons are concordant (<10% of discordance), however, five of them present high (>6%) ^{206}Pb of common origin and therefore were discarded. The detrital zircon age pattern is similar to that of the sample V11-170. In detail, the pattern comprises (Fig. 7c, Fig. A3 and Table 5): (1) a P1 population (52% of the pattern) virtually all composed of igneous grains from the morphological classes 1 and 3, and with ages between 512 Ma and 553 Ma with the youngest and major probability peak of the sample at 524 Ma; (2) a P2 population (13% of the pattern) of igneous and some metamorphic zircons from the morphological classes 2, 4, 5 and 6, in the range of 569–640 Ma and with a major probability peak at 602 Ma; (3) a P3 population (8% of the pattern) of igneous and metamorphic zircons from the morphological classes 3, 4, 6 and 7, and that range from 662 to 920 Ma with a major peak at 688 Ma; (4) a P4 population (20% of the pattern) of mainly igneous zircons from the morphological classes 2, 4, 5 and 7, and with ages of 963–1168 Ma and a major peak at 1030 Ma; (5) two populations of Paleoproterozoic (P5) and Archean (P6) ages. The youngest Unmix age of 516.8 ± 5.2 Ma (calculed from the P1 grains -youngest components-) suggest a Cambrian Epoch 2 or younger depositional age for the protolith of this metagreywacke from red lithofacies (Fig. 7c). This age is younger than the youngest probability peak of the sample at 524 Ma, because this peak represents both the youngest cluster of grain ages (Unmix age = 516.8 ± 5.2) and the contiguous groups with older ages.

6. Discussion

6.1. Depositional age of the siliciclastic protoliths of the Nahuel Niyeu Formation

The maximum depositional ages between 516.8 ± 5.2 Ma and 516.2 ± 4.5 Ma presented in this contribution (Fig. 7a, b and c) suggest a Cambrian Epoch 2 or younger depositional age for the siliciclastic protoliths of the three lithofacies of the Nahuel Niyeu Formation in Aguada Cecilio area. Upper limit for deposition is given by the crystallization age of 513.6 ± 3.3 Ma of the pre-kinematic sills intercalated in the metasedimentary sequence, whose injection occurred after the consolidation of the sedimentary sequence but previous to the onset of deformation and regional metamorphism (see Fig. 2; Greco et al., 2015). Therefore, deposition of siliciclastic protoliths of the Nahuel Niyeu Formation in the Aguada Cecilio area is narrowly constrained to the Cambrian Epoch 2 between 516.8–516.2 Ma and 513.6 Ma (Fig. 8). Furthermore, the closeness of the adjusted depositional age and maximum depositional ages signifies that the ages of the youngest detrital zircons effectively date the deposition of the siliciclastic protoliths of the Nahuel Niyeu Formation. Therefore, and adding into consideration maximum depositional ages from the area of Nahuel Niyeu to Valcheta (Figs. 1b and 9; sample NIY-012, 515 Ma, calculated from youngest probability peak, Pankhurst et al., 2006; samples SA108, 515 Ma and SA109, 507 Ma, calculated from youngest zircon grains, Rapalini et al., 2013), we propose a Cambrian Epoch 2 (probably during a time interval of ~520–510

	AGUADA CECILIO AREA	VALCHETA TO NAHUEL NIYEU AREA
Siliciclastic protoliths	Greyish green lithofacies: massive, laminated and foliated greywackes, and shales (***7***) Yellowish brown lithofacies: laminated greywackes and shales (***7***) Red lithofacies: massive and foliated greywackes, arenites, and shales (***7***) Texturally and compositionaly immature siliciclastic protoliths (***7***) Depositional age: between 516.8–516.2 Ma and 513.6 Ma (***7***) Gondwanan provenance of detrital zircons	Greywackes, shales and arenites (***1***, ***2***, ***3***, ***4***) Texturally and compositionaly immature siliciclastic protoliths (***2***, ***3, 4***) Maximum depositional age: 515–507 Ma (***5***, ***6***) Gondwanan provenance of detrital zircons (***6***)
	Depostional age of the siliciclastic protoliths of the entire Nahuel Niyeu Formation during the Cambrian Epoch 2 (~520–510 Ma) (***7***)	
	Source rocks (forming part of a same proximal source area) (***7***): (1) 520–510 Ma acidic volcanic rocks representing an active magmatic arc (2) ~555–>520 Ma acidic plutonic and volcanic rocks representing earlier stages of probably the same active magmatic arc (3) Low to high-grade, paraderived metamorphic rocks with deposition and regional metamorphism during the latest Ediacaran–Terreneuvian interval, representing the country rocks of the arc	

Sources:
Caminos, 1983 (***1***), 2001(***2***), Caminos and Llambías, 1984 (***3***); Cagnoni et al., 1993 (***4***); Pankhurst et al., 2006 (***5***); Rapalini et al., 2013 (***6***); this contribution (***7***)

Fig. 8. Simplified and comparative chart of the sedimentary protolith characteristics of the Nahuel Niyeu Formation.

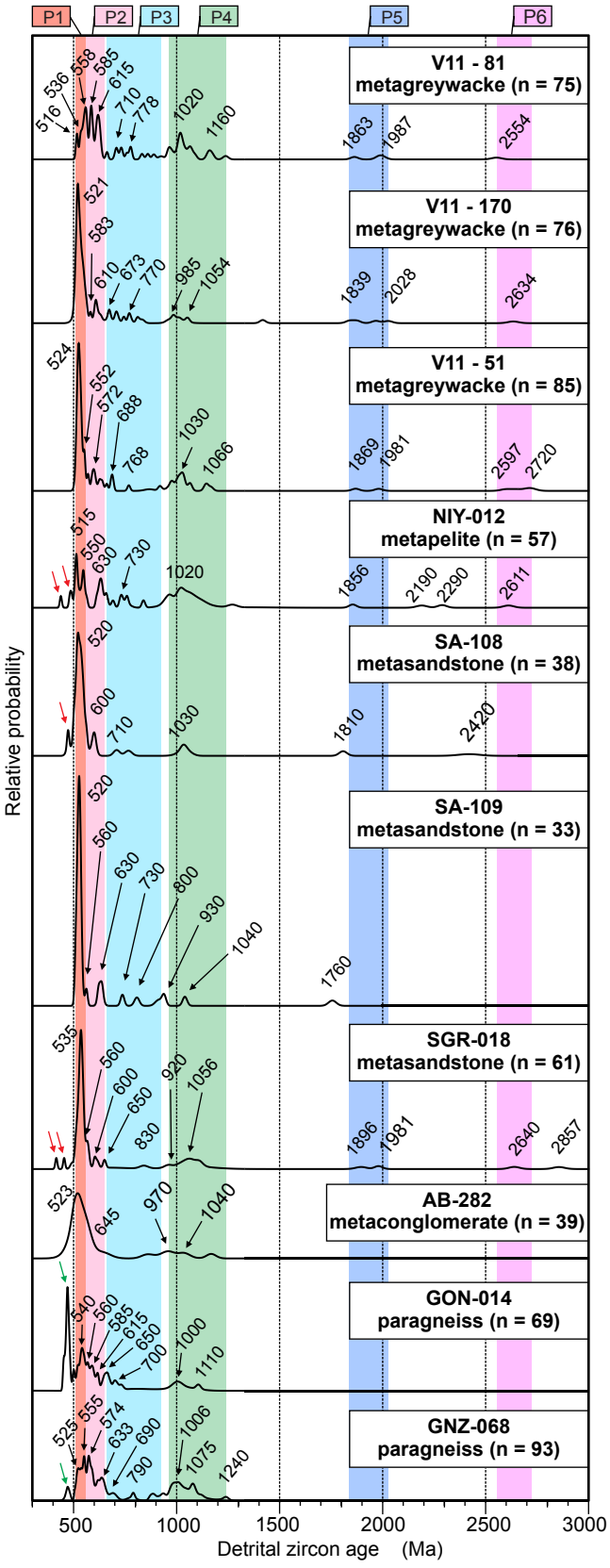

Fig. 9. Normalized relative probability plots of detrital zircon ages of metamorphic rocks, derived from siliciclastic protoliths, from the basement units of the eastern North Patagonian Massif. Samples correspond to the Nahuel Niyeu Formation (V11-81, V11-170 and V11-51, this contribution; NIY-012, Pankhurst et al., 2006; SA-108 and SA-109, Rapalini et al., 2013), the El Jagüelito Formation (SGR-018, Pankhurst et al., 2006; AB-282, Naipauer et al., 2010) and the Mina Gonzalito Complex (GON-014, Pankhurst et al., 2006; GNZ-068, Greco et al., 2014). The younger probability peak of the sample GON-14 and GNZ-068 (green arrows) results from analyses executed over zircon rims that grew during metamorphism of the Mina Gonzalito Complex. Red arrows mark data reflecting Pb-loss, as indicated the authors. Numbers over the curves are the ages of probability peaks. n = total analyzed grains. Color bars are the same as in Fig. 7 and represent the ages of the populations of zircon grains established for the Nahuel Niyeu Formation. Samples localities are in Fig. 1. (For interpretation of the references to colour in this figure legend, the reader is referred to the web version of this article.)

Ma) depositional age for the siliciclastic protoliths of the entire Nahuel Niyeu Formation (Fig. 8).

6.2. Maturity of the siliciclastic protoliths of the Nahuel Niyeu Formation

The global analysis of the relict sedimentary features and the morphological characteristics and origin of the detrital zircons from the metasandstones of the Nahuel Niyeu Formation in the Aguada Cecilio area provide valuable information about the maturity of the siliciclastic protoliths and the proximity of the source rocks to the basin.

At this respect, the poorly sorted, angular to subrounded detritus and the abundant, recrystallized fine matrix preserved in the metagreywackes of the three lithofacies (the most typical lithology in the Aguada Cecilio area) suggest texturally immature siliciclastic protoliths (e.g. Figs. 5a–f; 6a–e), following the concept of Folk (1951). The coexistence of detrital zircon grains of different morphological classes in the three analyzed metagreywackes also reflects texturally immature protoliths (Table 2). In addition, the abundant labile detrital grains of plagioclase, alkali feldspar and lithic fragments recognized in the metagreywackes and metaarenites of the three lithofacies (Figs. 5a–f and 6a–f) reveal that the siliciclastic protoliths were also compositionally immature. Similar relict sedimentary features indicating texturally and compositionally immature protoliths were also described in metagreywackes of this unit from south of Nahuel Niyeu (Caminos and Llambías, 1984; Cagnoni et al., 1993; Caminos, 2001).

Texturally immature sediments have not undergone sufficient transport and reworking to remove fine size material and produce sorting and rounding of detritus, prior to their deposition (Boggs, 2009, p. 52). Moreover, compositionally immature sediments are typically deposited close to their source area or they have been rapidly transported and deposited with little reworking from a source area with limited physical and chemical weathering (Tucker, 2001, p. 48). Hence, we consider that the texturally and compositionally immature protoliths of the Nahuel Niyeu Formation were derived from proximal sources (Fig. 8).

6.3. Composition and age of the proximal sources of the siliciclastic protoliths of the Nahuel Niyeu Formation

The relict detrital composition of the metasandstones of the three lithofacies of the Aguada Cecilio area suggests that the proximal sources of the siliciclastic protoliths of the Nahuel Niyeu Formation were composed of acidic volcanic and plutonic rocks associated with low- to high-grade metamorphic rocks. Furthermore, the metamorphic lithic fragments of phyllite and polycrystalline quartz preserved in the metasandstones might indicate that the metamorphic sources were composed mainly of paraderived metamorphic rocks. In addition, igneous and metamorphic detrital zircon grains in the analyzed metagreywackes reflect all these sources. Our findings about the composition of the sources are similar to those reported in previous petrographical and geochemical studies for the siliciclastic protoliths of this unit, south

of Nahuel Niyeu (Caminos and Llambías, 1984; Cagnoni et al., 1993; Caminos, 2001).

Bearing in mind the established sources, we analyze below the detrital zircon populations of our samples in order to assess the ages of these sources.

The youngest detrital zircons of igneous origin (with ages equal and younger than 520 Ma) within the P1 populations recorded in the analyzed metagreywackes (Figs. A1, A2 and A3; Tables 3, 4, 5, A1, A2 and A3) suggest that the proximal, acidic igneous sources resulted in part from a syndepositional igneous activity. In addition, detrital zircons with equivalent ages also are present in the samples from the area of Nahuel Niyeu to Valcheta (Figs. 1b and 9; NIY-012, SA108 and SA109) analyzed by Pankhurst et al. (2006) and Rapalini et al. (2013). The metatuffs of the red lithofacies (Fig. 3f) and the geochemical characteristics of the pre-kinematic sills (see Section 3.1.2) suggest that the syndepositional igneous activity would have been associated with an active magmatic arc developed over continental crust. The different proportions in which these youngest grains appear in the analyzed metagreywackes might reflect a strong or restricted supply from this active arc (sample V11-81, restricted supply; samples V11-170 and V11-51, strong supply). This active magmatic arc probably supplied the youngest zircons and part of the acidic volcanic detritus mainly from the surficial volcanic cover. Similarly, Pankhurst et al. (2006) indicated that the dominance of the youngest peak at ca. 515 in their sample (Fig. 9; sample NIY-012) suggests erosion from a nearby active arc.

The detrital zircons with igneous origin and ages between 556 and >520 Ma in the P1 population of the three analyzed metagreywackes allow us to infer proximal, acidic plutonic and volcanic sources with these ages (Figs. A1, A2 and A3; Tables 3, 4, 5, A1, A2 and A3). These detrital zircon grains are dominant in the samples V11-170 and V11-51 suggesting strong supply from these igneous sources. By contrast, igneous zircon grains with these ages are scarce in the sample V11-81, implying restricted supply from these igneous sources. Rocks resulted from an igneous activity coeval with the Tardugno Granodiorite, which have crystallization ages between 528 and 522 Ma (Fig. 1b; Rapalini et al., 2013; Pankhurst et al., 2014), might have been the source of the igneous detrital zircon grains with ages between ~530 and >520 Ma. The Tardugno granodiorite is a direct plutonic evidence of arc magmatism during the Terreneuvian (Rapalini et al., 2013; Pankhurst et al., 2014). Thus, the igneous sources with ages of 556 to >520 Ma might represent earlier stages of the same active magmatic arc (older than and coeval with the emplacement of the Tardugno Granodiorite and lasting up to the Cambrian Epoch 2). Rapalini et al. (2013) also assigned a large number of Early Cambrian detrital zircons from the samples SA-108 and SA-109 to local sources.

The distributions of older detrital zircon ages in our samples (P2 to P6) are similar to those of corresponding detrital zircon ages reported by Pankhurst et al. (2006) and Rapalini et al. (2013) (Samples NIY-012, SA-108 and SA-109, Figs. 7a, b, c and 9). Pankhurst et al. (2006) described their distribution of older detrital zircon ages as a typically Gondwanan. In addition, inherited zircon cores from the Terreneuvian Tardugno Granodiorite, recording Neoproterozoic, Mesoproterozoic and Paleoproterozoic U–Pb ages, were interpreted as incorporated from an Eocambrian or late Neoproterozoic sediment or metasediment representing polyrecycled Gondwana margin material in the upper crust (Fig. 10, sample VAL010, SHRIMP U–Pb zircon Pankhurst et al., 2014). Although the ages of the inherited zircon cores represent probably an incomplete detrital zircon age pattern of the source material, they are equivalent to those of the older populations of the Nahuel Niyeu Formation (cf. Figs. 9 and 10). Furthermore, undated schists of the Yaminué Complex cropping out north of the Tardugno Granodiorite (Fig. 1a) probably represent the country rock of this

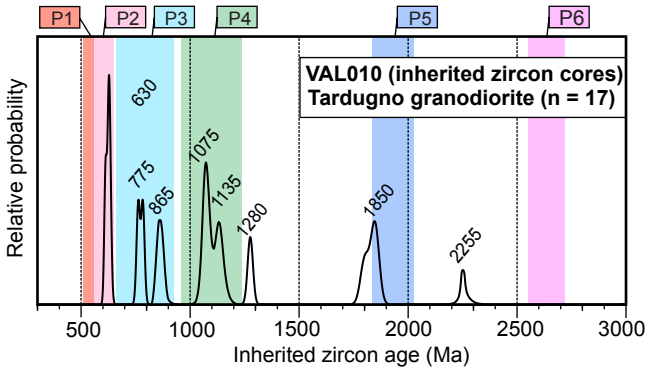

Fig. 10. Relative probability plot of inherited zircon cores from the Tardugno Granodiorite (Sample VAL010, Pankhurst et al., 2006). Two Cambrian inherited zircon cores dated at 545 and 528 Ma interpreted as products of local isotopic homogenization by the authors are not plotted. Numbers over the curves are the ages of probability peaks. n = total analyzed grains. Color bars are the same as in Fig. 7 and 9 and represent the ages of the populations of zircon grains established for the Nahuel Niyeu Formation (P1–P6). The sample corresponds to the outcrops located south of Nahuel Niyeu (Fig. 1). Exact location is in Pankhurst et al. (2006). (For interpretation of the references to colour in this figure legend, the reader is referred to the web version of this article.)

igneous body (Chernicoff and Caminos, 1996b; von Gosen, 2003) and might represent an outcrop of the source of their inherited zircon cores. The schists are lithologically comparable to the metamorphic lithic fragments (polycrystalline quartz) recorded in the metasandstones rocks of the Nahuel Niyeu Formation. The equivalence between the above zircon ages and this lithological comparison allow us to consider that rocks equivalent to the country rock of the Tardugno Granodiorite might have been the paraderived metamorphic sources established for the siliciclastic protoliths of the Nahuel Niyeu Formation. Thus, these sources would have supplied the older populations (P2 to P6) of detrital zircons recorded in the Nahuel Niyeu Formation. In addition, the youngest detrital zircons of metamorphic origin with ages of 538 to 530 Ma within the P1 population recorded in our samples (Tables A1, A2 and A3) suggest a regional metamorphic event occurred during Terreneuvian. Accordingly, the paraderived metamorphic sources and part of the older igneous sources probably underwent this event.

The paraderived metamorphic source rocks would have been the main source of the analyzed metagreywacke from the greyish green lithofacies (sample V11-81) because of their P2, P3, P4, P5 and P6 detrital zircon populations accumulate 83% of the detrital zircon age pattern (Table 3). By contrast, the P2, P3, P4, P5 and P6 detrital zircon populations of the analyzed metagreywackes from the yellowish brown (sample V11-170) and red (sample V11-51) lithofacies accumulate 48 and 42%, respectively (Tables 4 and 5), suggesting that the paraderived metamorphic source were secondary in relation to the igneous sources younger than 556 Ma.

According to the lithological features and the analysis of the detrital zircon populations discussed before, the most likely proximal source rocks of the compositionally and texturally immature siliciclastic protoliths of the Nahuel Niyeu Formation were three (Fig. 8): (1) 520–510 Ma, acidic volcanic rocks representing an active magmatic arc, (2) ~555–>520 Ma, acidic plutonic and volcanic rocks representing earlier stages of the same active magmatic arc, and (3) low to high-grade, paraderived metamorphic rocks with deposition and regional metamorphism during the latest Ediacaran–Terreneuvian interval, representing the country rocks of the arc. This interpretation implies that all these source rocks probably formed part of a same proximal source area. Mixing in different proportion of detritus from the three types of sources

would give any of the patterns of detrital zircon ages recognized in the Nahuel Niyeu Formation.

6.4. Comparison of the protoliths of the metamorphic basement units of the eastern North Patagonian Massif

In order to contribute to regional correlations from the point of view of the protoliths of the metamorphic basement units of the eastern North Patagonian Massif, we compare the Nahuel Niyeu and El Jagüelito formation and the Mina Gonzalito Complex putting emphasis on the primary features of the paraderived metamorphic rocks derived from siliciclastic protoliths. The comparison also includes the orthoderived metamorphic rocks intercalated in the paraderived metamorphic sequences. These rocks are those whose igneous protolith emplacement occurred during deposition of the siliciclastic protoliths, or after lithification but before the onset of deformation and regional metamorphism of these units. Fig. 11 summarizes the comparison and the available lithological and geochronological data of these metamorphic units.

The low-grade Nahuel Niyeu and El Jagüelito formations have been compared on the basis of similar lithology and metamorphic grade (Caminos and Llambías, 1984; Giacosa, 1987; von Gosen, 2003; Greco et al., 2015). Geochemical studies of the El Jagüelito Formation (Giacosa, 1997; Dalla Salda et al., 2003a), added to detrital grains of granitoids, intermediate to acidic volcanic rocks, polycrystalline quartz, metapelites and schists preserved in metasandstones and metaconglomerates of this unit (Braitsch, 1965; González et al., 2011b), suggest igneous and metamorphic sources related to an active continental margin for the siliciclastic protoliths, like those of the Nahuel Niyeu Formation. Metagreywackes, lithic metaarenites and minor polymictic metaconglomerates of the El Jagüelito Formation demonstrate the immature nature of it siliciclastic protoliths, probably implying proximal sources, as in the Nahuel Niyeu Formation. Additionally, igneous and metamorphic detrital zircons from paragneisses of the Mina Gonzalito Complex (Pankhurst et al., 2006) indicate igneous and metamorphic sources for its siliciclastic protoliths, as in the Nahuel Niyeu and El Jagüelito formations. Moreover, the similar detrital zircon pattern in the three basement units also suggests equivalent source rocks (Fig. 9).

The siliciclastic protoliths of the three basement units were also compared on the basis of similar Cambrian maximum depositional ages and detrital zircon patterns (Pankhurst et al., 2006; Naipauer et al., 2010; Martínez Dopico et al., 2011; Rapalini et al., 2013; Greco et al., 2014, 2015). The maximum depositional ages between 516.8 and 516.2 Ma and the detrital zircon patterns of our samples from the Nahuel Niyeu Formation in Aguada Cecilio area

		NAHUEL NIYEU FORMATION	EL JAGÜELITO FORMATION	MINA GONZALITO COMPLEX
Paraderived metamorphic rocks	**Lithology**	Metagreywackes, phyllites and minor metaarenites (***1***, ***2***, ***3***, ***4***, ***5***, ***6***, ***7***) Texturally and compositionally, immature siliciclastic protoliths: greywackes, shales and minor arenites (***2***, ***4***, ***7***)	Metagreywackes, slate, phyllite, metaarenites and minor metaconglomerates (***1***, ***2***, ***3***, ***4***, ***5***, ***6***, ***7***, ***8***, ***9***,***10***, ***11***. ***12***) Texturally and compositionally, immature siliciclastic protoliths: greywackes, shales, arenites and minor conglomerates (***3***, ***8***, ***10***, ***12***)	Paragneisses, schists, migmatites and minor marbles (***1, 2, 3, 4***) Protoliths: siliciclastic rocks (metasandtone and shale) and minor limestones (***4***)
	Detrital zircon data	Maximum depositional ages of 516.8–516.2 Ma (Aguada Cecilio area, ***7***) and 515–507 Ma (south of Nahuel Niyeu and west of Valcheta***; 8, 9***) Gondwanan provenance (***7***, ***8***, ***9***)	Maximum depositional ages of 535 Ma and 523 Ma ***(13***, ***14***), consistent with ages indicated by trace fossils (***6***) and Archeocyath fossils (***9***) Gondwanan provenance ***(13***, ***14***)	Maximum depositional ages of 540-535 Ma and 515 Ma ***(5, 6***), coherent with depositional ages of marbles protoliths of *ca*. 550–510 Ma (***7***) Gondwanan provenance ***(5, 6***)
	Source rocks of siliciclastic protoliths	Source rocks (forming part of a same proximal source area) (***7***): (1) 520–510 Ma acidic volcanic rocks representing an active magmatic arc (2) ~555–>520 Ma acidic plutonic and volcanic rocks representing earlier stages of the same active magmatic arc (3) Low/high-grade, paraderived metamorphic rocks with deposition and regional metamorphism during the latest Ediacaran–Terreneuvian interval, representing the country rocks of the arc		
Orthoderived metamorphic rocks (intercalated in the paraderived metamorphic rocks)		Dominantly metagabbro/dioritic sills with subduction-related tholeiitic signature; metaandesite lava flow (***6***); metatuffs Magmatic crystallization of the sills: 513.6 ± 3.3 Ma (***6***)	Metatuffs, metaignimbrites, metaandedesite and metarhyolite lava flows, and metarhyolitic dikes and domes; calc-alkaline geochemical signature (***10***)	Amphibolites (***4***)
Tectonic setting of sedimentary and igneous protoliths		Convergent continental margin basin associated with an active magmatic arc (***6***) (*Nahuel Niyeu basin*, ***7***), developed during the Cambrian Epoch 2 (~520–510 Ma, ***7***); probably a forearc basin related to an extensional tectonic regime (***7***)		

Sources:
Nahuel Niyeu Formation: Caminos, 1983 (***1***), 2001 (***2***), Caminos and Llambías, 1984 (***3***); Cagnoni et al., 1993 (***4***); Giacosa, 1999 (***5***); Greco et al., 2015 (***6***); This contribution (***7***); Pankhurst et al., 2006 (***8***); Rapalini et al., 2013 (***9***).
El Jagüelito Formation: de Alba, 1964 (***1***); Giacosa, 1987 (***2***), 1997 (***3***); Giacosa and Paredes, 2001 (***4***); von Gosen, 2002 (***5***); González et al., 2002 (***6***), 2008b (***7***), 2011b (***8***), a (***9***), 2013 (***10***); González P.D. et al., 2014 (***11***); Dalla Salda et al., 2003b (***12***); Pankhurst et al., 2006 (***13***); Naipauer et al., 2010 (***14***).
Mina Gonzalito Complex: Ramos, 1975 (***1***); Giacosa, 1987 (***2***), 1997 (***3***); González et al., 2008a (***4***); Pankhurst et al., 2006 (***5***); Greco et al., 2014 (***6***); Varela et al., 2014 (***7***).

Fig. 11. Simplified and comparative chart of the paraderived and orthoderived metamorphic rocks of the Nahuel Niyeu and El Jagüelito formations and the Mina Gonzalito Complex.

are consistent with the published data. Particularly, the youngest maximum depositional ages of the Mina Gonzalito Complex (Figs. 1c, d, and 9; sample GNZ-068, 515 Ma, weighted-mean age of the youngest discrete population of detrital zircons) and the El Jagüelito Formation (sample AB-282, 523 Ma, youngest probability peak) better constrain this parameter and are similar to our maximum depositional ages. Maximum depositional ages of the siliciclastic protoliths of the three basement units are coherent with the age indicated by the archeocyath fossils (between 521 and ~513 Ma) contained in limestone blocks of a metaconglomerate of the El Jagüelito Formation (González et al., 2011b) and the depositional age of ca. 550–510 Ma of the marble protoliths from the Mina Gonzalito Complex obtained from strontium isotopic studies (Varela et al., 2014).

Upper limit for deposition of the siliciclastic protoliths of the El Jagüelito Formation is given by conventional and SHRIMP U–Pb zircon crystallization ages of 476 Ma of granitoids of the Punta Sierra Plutonic Complex (Varela et al., 1998; Pankhurst et al., 2006). In the case of the Mina Gonzalito Complex, upper limit for deposition of their sedimentary protoliths (siliciclastic rocks limestones) is defined by the SHRIMP U–Pb zircon crystallization age of 492 Ma of the granodioritic orthogneiss of this complex (González et al., 2008a; Varela et al., 2011a). These upper limits and the maximum depositional ages both the El Jagüelito Formation and Mina Gonzalito Complex are consistent with the depositional age assigned to the Nahuel Niyeu Formation. Therefore and considering the previously depicted similarities, deposition of the siliciclastic protoliths of the three basement units might have been coeval (~520–510 Ma, Cambrian Epoch 2).

With regard to the orthoderived metamorphic rocks intercalated in the paraderived metamorphic sequences, the Nahuel Niyeu Formation shows the dominantly, metagabbro/dioritic pre-kinematic sills with a subduction-related tholeiitic signature, the metaandesitic lava flow and the metatuffs. Amphibolite layers intercalated in the paragneisses and schists of the Mina Gonzalito Complex were interpreted as pre-kinematic, mafic igneous flows (González et al., 2008a), and also considered as the higher metamorphic equivalents of the sills and the lava flow of the Nahuel Niyeu Formation (Greco et al., 2015). In contrast, the El Jagüelito Formation exhibits intercalations of metatuffs, metaignimbrites, metaandedesitic and metarhyolitic lava flows, as well as some metarhyolitic dikes and domes, all of them with a calc-alkaline geochemical signature (González et al., 2013). These mainly acidic metaigneous rocks have a calc-alkaline geochemical signature suggesting derivation from a proximal, active magmatic arc (González et al., 2013). This arc might have been the same that we interpreted as representing the 520–510 Ma, acidic volcanic sources of the siliciclastic protoliths of the Nahuel Niyeu Formation. Despite the compositional differences, the geochemical signature indicates subduction related magmatism for the igneous protoliths of the orthoderived metamorphic rocks of all basement units.

6.5. *Tectonic setting of the protoliths of the Nahuel Niyeu and El Jagüelito formations and the Mina Gonzalito Complex: the Nahuel Niyeu basin*

Previous petrographical, geochronological and geochemical studies have shown that both the siliciclastic and intercalated igneous protoliths of the Nahuel Niyeu and El Jagüelito formations and the Mina Gonzalito Complex were related to a convergent continental margin associated with active arc magmatism (Cagnoni et al., 1993; Giacosa, 1997; Dalla Salda et al., 2003a; Pankhurst et al., 2006; González et al., 2013; Greco et al., 2015). Furthermore, Greco et al. (2015) suggested that the protoliths of the three units filled a basin associated with this tectonic setting, during the Early Cambrian. These authors linked this basin to the Terra Australis Orogen of the south Gondwana margin (Cawood, 2005), adding to Pankhurst et al. (2006) that considered the siliciclastic protoliths of the three basement units as deposited on a continental shelf at this margin on the basis of similar Gondwanan provenance patterns of their samples. In contrast to the above studies, Ramos and Naipauer (2014) interpreted a collisional continental margin as tectonic setting for the protoliths.

In addition, detrital zircon patterns of almost all samples from these metamorphic units suggest deposition of the siliciclastic protoliths in convergent basins (e.g. trench, forearc, intra-arc and backarc basins), according to the model of Cawood et al. (2012) (Fig. 12), in agreement with those previous studies indicating a similar tectonic setting. This is an interesting finding because it, added to results of the comparison of Section 6.4, argues for the basin proposed by Greco et al. (2015). Moreover, the results of this comparison suggests that this basin would have developed during the Cambrian Epoch 2 (~520–510 Ma), receiving detritus mainly from the proximal source area established for the siliciclastic protoliths of the Nahuel Niyeu Formation (Fig. 11). This basin was probably a key tectonic element in this region of the south Gondwana margin, and thus, we suggest to name it as “Nahuel Niyeu basin”. The outcrops of the Nahuel Niyeu and El Jagüelito formations and the Mina Gonzalito Complex would represent part of the Nahuel Niyeu basin, after deformation and regional metamorphism.

6.6. *Position of the source area of the Nahuel Niyeu basin: interpreting the type of basin*

In this section, we analyze the position of the proximal source

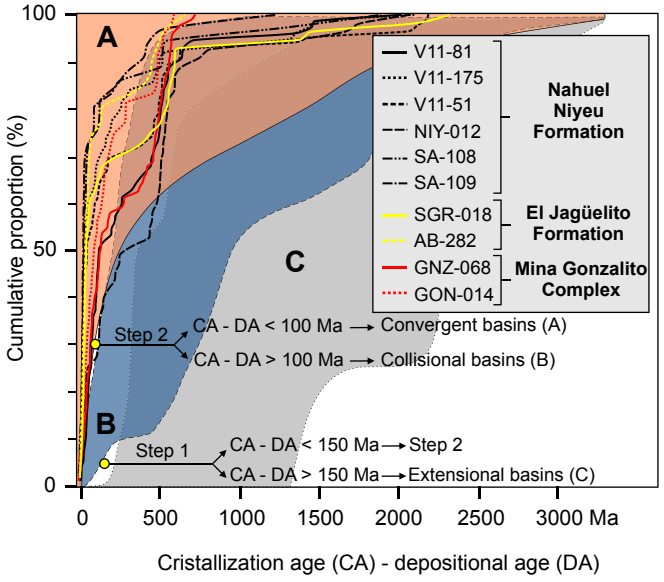

Fig. 12. Distribution of the difference between the measured crystallization age (CA) of each detrital zircon grain and the depositional age (DA) of the siliciclastic protoliths of the Nahuel Niyeu and El Jagüelito formations and the Mina Gonzalito Complex (after Cawood et al., 2012). The distribution is plotted as cumulative proportion curves. To simplify, we adopted a depositional age of 515 Ma (a mean between 520 and 510 Ma, which is the interval of time of probably deposition for the siliciclastic protoliths of the Nahuel Niyeu basin, see sections 6.3 and 6.4). Color shaded fields represent convergent (A: brown), collisional (B: blue) and extensional (C: grey) basins. Extensional basins have CA – DA greater than 150 Ma in the youngest 5% of the zircons (step 1). Convergent basins have CA – DA less than 100 Ma in the youngest 30% of zircons (step 2). Collisional basins have CA – DA greater than 100 Ma in the youngest 30% of zircons (step 2). Almost all samples fall in the field of the convergent basins. The samples are the same as in Fig. 9. (For interpretation of the references to colour in this figure legend, the reader is referred to the web version of this article.)

area of the Nahuel Niyeu basin. This area would include igneous rocks of both the active magmatic arc associated with the basin and the earlier stages of this arc, as well as the metamorphic country rocks of the arc (Fig. 11). Our analysis allow us to interpret the position of the basin within the convergent continental margin where it was probably developed, providing a better understanding of this tectonic setting.

The ~NW–SE trend of the belt along which the Nahuel Niyeu and El Jagüelito formations and the Mina Gonzalito Complex crop out might indicate that the Nahuel Niyeu basin was elongated in this direction (present coordinates), despite deformational and metamorphic overprint (Figs. 1b–d and 13). Generally, most basins associated with convergent continental margins are elongated parallel to the trench and related magmatic arc (Underwood and Moore, 1995; Smith and Landis, 1995; Marsaglia, 1995; Jordan, 1995; Dickinson, 1995). Therefore, the proximal source area of the Nahuel Niyeu basin should have been toward either the southwestern or the northeastern side of the basin, and close to it. Additionally, the outcrops of the Tardugno Granodiorite and its country rock, both along the long axis of the basin and controlled by late Paleozoic SE-directed reverse faults (Figs. 1b and 13), suggests that these rocks might have been part of the substratum of this basin. Therefore, rocks representing the earlier stages of the active magmatic arc and its country rocks might have been part of both the proximal source area and the substratum of the basin.

Toward the SW of the basement outcrops of the eastern North Patagonian Massif, igneous and metamorphic rocks that can represent the proximal source area of the Nahuel Niyeu basin have not been recorded, neither in the southwestern North Patagonian Massif nor in the North Patagonian Cordillera. There, the oldest igneous rocks are granitoids with latest Silurian to Devonian U–Pb zircon crystallization ages (Varela et al., 2005; Pankhurst et al., 2006; Hervé et al., 2016). Besides, protoliths of paraderived metamorphic rocks have Cambrian Epoch 3 (Serra-Varela et al., 2016), Silurian and Visean (Hervé et al., 2005, 2016) maximum depositional ages. All these data are younger than the sources of the basin. Therefore, the proximal source area of the basin might have been located toward the NE of the outcrops of the Nahuel Niyeu and El Jaguelito formations and the Mina Gonzalito Complex.

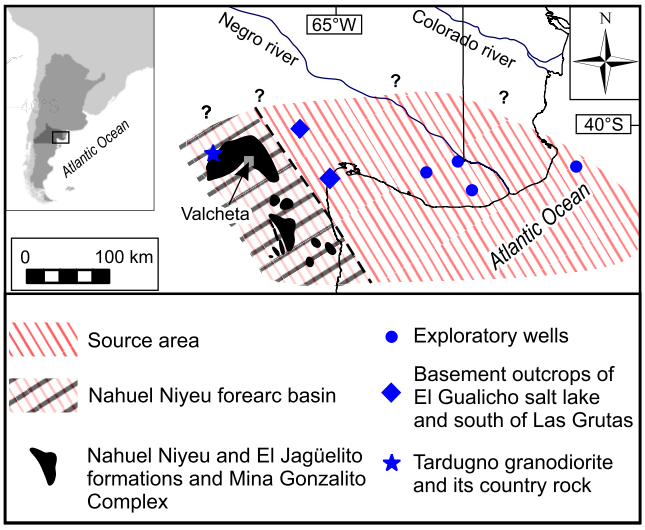

Fig. 13. Proposed location of the Nahuel Niyeu forearc basin and its proximal source area. The limit between them (dotted line) might partially correspond to a lineament of steep gravity gradient in this region (lineament "D" in Gregori et al., 2008). Basement rocks from El Gualicho salt lake, south of Las Grutas and exploratory wells might represent part of the sources of the Nahuel Niyeu basin. The Tardugno granodiorite and its country rock are interpreted as part of the substratum of the basin. The outcrops of the Nahuel Niyeu and El Jagüelito formations and the Mina Gonzalito Complex would represent part of the Nahuel Niyeu basin, after deformation and regional metamorphism.

Toward the NE of the outcrops of the Nahuel Niyeu and El Jagüelito formations and the Mina Gonzalito Complex, igneous and high-grade, para- and ortoderived metamorphic rocks of the Las Grutas igneous-metamorphic complex (Sato et al., 1998) crop out in small and scattered areas south of Las Grutas (Figs. 1 and 13). Besides, low to medium-grade, paraderived metamorphic rocks were discovered at onshore and offshore exploratory wells (Kaasschieter, 1965; Zambrano, 1980). The rocks from the Las Grutas igneous-metamorphic complex and the exploratory wells are lithologycally comparable to the proximal sources of the basin, however, they lack robust geochronological data that reveal their age. Despite this limitation, and according to the above discussion, we suggest that these basement rocks might represent part of the sources of the Nahuel Niyeu basin. In addition, the low-grade metasedimentary rocks near the Gualicho salt lake, located toward the NE of the Nahuel Niyeu area, are also lithologycally comparable to the basin sources. Although they were considered as belonging to the Nahuel Niyeu Formation (Caminos and Llambías, 1984), this correlation is only based on similar lithology and lacking geochronological data that confirm or not it. Hence, they might also represent part of the source rocks of the basin. In summary, we propose the area where all these basement rocks are located as the proximal source area of the Nahuel Niyeu basin (Fig. 13). Accordingly, we interpret that the limit between the basin and its source area might partially correspond to a lineament of steep gravity gradient in this region (lineament "D" in Gregori et al., 2008). The proposal implies that young sedimentary rocks and sediments, both onshore in the area of the Negro river and offshore in the Atlantic Platform, would currently cover most rocks representing the proximal sources of the basin.

Considering the interpreted position of the proximal source area of the Nahuel Niyeu basin, and a landward-dipping subduction of the paleo-Pacific Ocean beneath the southern margin of Gondwana during the Cambrian (e.g. Curtis, 2001; Cawood, 2005; Cawood and Buchan, 2007; Schwartz et al., 2008; Tohver et al., 2012), we suggest that this basin probably was a forearc basin (Fig. 14).

In addition, it is interesting to examine several aspects of forearc basins in order to compare them with the Nahuel Niyeu basin and add more information to it. At this respect, forearc basins fill consist mainly of siliciclastic immature deposits, dominantly interbedded sandstone and shale with conglomerate intervals, typically derived from the associated volcanic arc and its roots and paraderived metamorphic country rocks of this arc (Dickinson, 1995; Dickinson and Seely, 1979). This is a similar situation to that of the Nahuel Niyeu basin (Fig. 11). Moreover, the strata of the inner edge of forearc basins may interfinger with volcanic and pyroclastic rocks derived from the arc (Dickinson and Seely, 1979; Trop et al., 2003). This is particularly comparable with the calc-alkaline metaigneous rocks interbedded with the metasedimentary rocks of the El Jagüelito Formation, and therefore, the protoliths of this unit might correspond with the inner edge of the Nahuel Niyeu basin (Fig. 14). Basaltic sills with subduction-related tholeiitic signature, like those of the Nahuel Niyeu Formation and the Mina Gonzalito Complex, are a common feature in forearc basins associated with an extensional regime, particularly in their outer and central zones (Fig. 14; Marlow et al., 1992a, 1992b; Bloomer et al., 1994; Taylor et al., 1995; Sánchez Lorda et al., 2014). Additionally, carbonate platforms, as that interpreted for protoliths of the marbles of the Mina Gonzalito Complex (Dalla Salda et al., 2003b), are also common in forearc basins, mainly in their inner edge and over the subduction

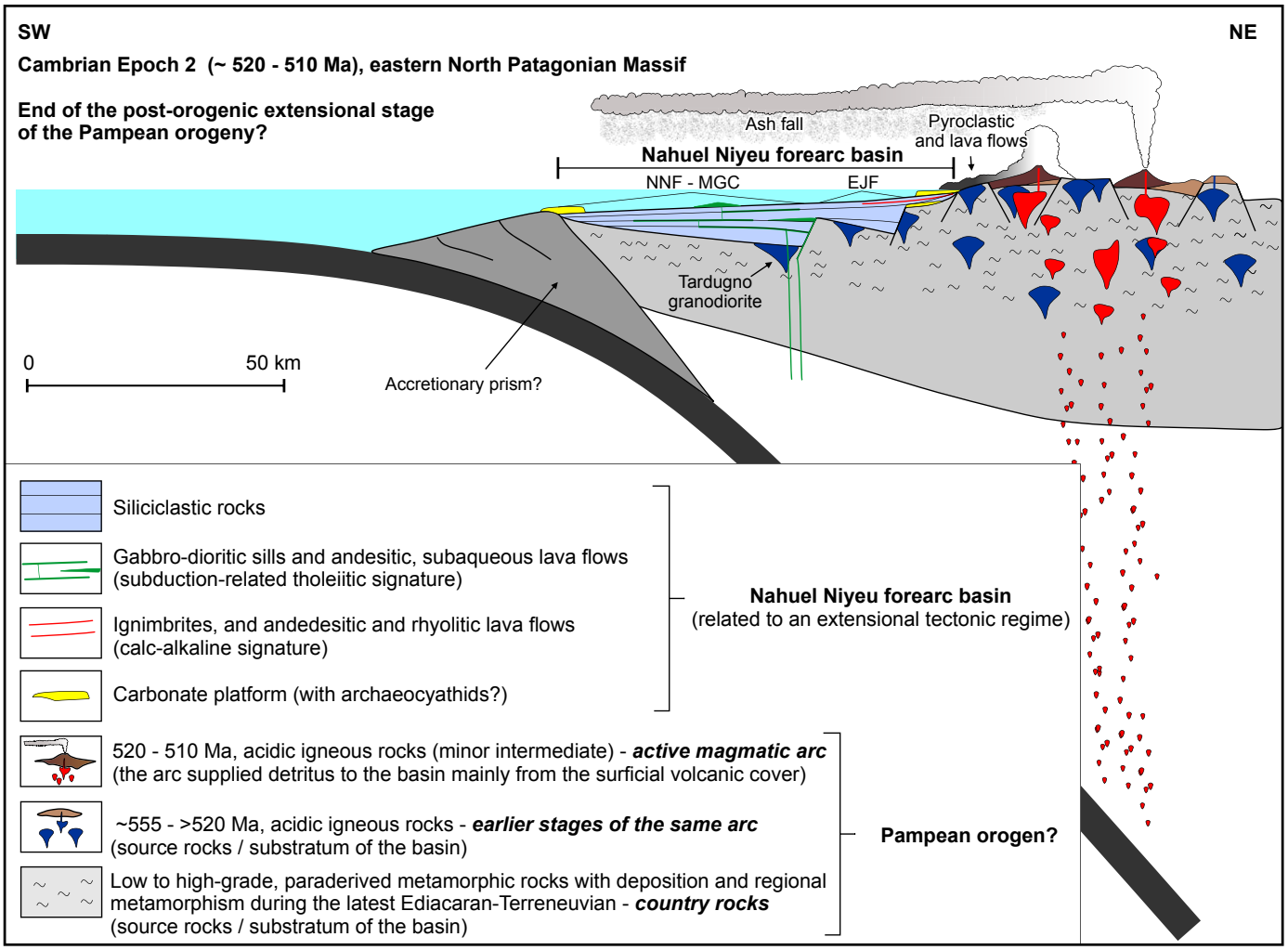

Fig. 14. Schematic sketch of the Nahuel Niyeu forearc basin oriented with present coordinates. Abbreviations: NNF (Nahuel Niyeu Formation), MGC (Mina Gonzalito Complex) and EJF (El Jagüelito Formation). Tuffs from the active magmatic arc are widely distributed in the basin. Note the possible position of the protoliths of the metamorphic units within the basin. The accretionary prism is interpretative.

complexes and the distal part of these basins (Fig. 14; Dorobek, 2008). The age of the archaeocyath fossils (between 521 and ~513 Ma) contained in limestone blocks of a metaconglomerate of the El Jagüelito Formation indicates that deposition of this limestone was virtually contemporaneous with the siliciclastic deposition in the Nahuel Niyeu forearc basin. Thus, and considering the previously suggested location of the protoliths of this formation in the basin, the limestone might be interpreted as derived from a local carbonate platform in the inner edge of the basin (Fig. 14). In this case, it might be equivalent to that interpreted in the Mina Gonzalito Complex, the latter suggested as the source of the limestone blocks (González et al., 2011b). Further, the protolith of the metaconglomerate might represent a debris flow originated in the source area, eroding the inner edge carbonate platform and incorporating their blocks, and probably confined to submarine or fluviodeltaic channels, which are common in forearc basins (Dickinson, 1995). In summary, all the previously examined aspects support the Nahuel Niyeu basin as a forearc basin. Furthermore, some aspects allow to infer the possible position of the protoliths of the metamorphic units within the basin (e.g. Nahuel Niyeu Formation and Mina Gonzalito Complex in the outer and central zone) and an extensional tectonic regime associated with the basin (Fig. 14).

6.7. Implications for northern Patagonia in the context of the southern margin of Gondwana

Several contributions have postulated different alternatives for the origin of Patagonia and its evolution in the southern margin of Gondwana, during the Paleozoic. Following, we examine only those alternatives that involve the origin and evolution of the North Patagonian Massif.

The hypothesis of an allochthonous Patagonia implies a Carboniferous–Early Permian subduction-related magmatic arc along the northern part of the North Patagonian Massif, which was associated with the consumption of an ocean between South America and Patagonia as an amalgamated terrane, and a subsequent collision in the Early–Middle Permian related to the Gondwanide orogen (Ramos, 1984, 2008). The collision was along a potential suture coinciding in part with the right-lateral, strike-slip Huincul fault and a magnetic anomaly buried below the Colorado basin (Fig. 1a; Ramos, 2008 and references therein). It causes NE-vergent deformation in Sierras Australes and SW-vergent thrusting in northern Patagonia (von Gosen, 2003 and references therein).

The hypothesis of an allochthonous Patagonia was reinforced by other researchers that have argued for an Antarctic–Patagonia

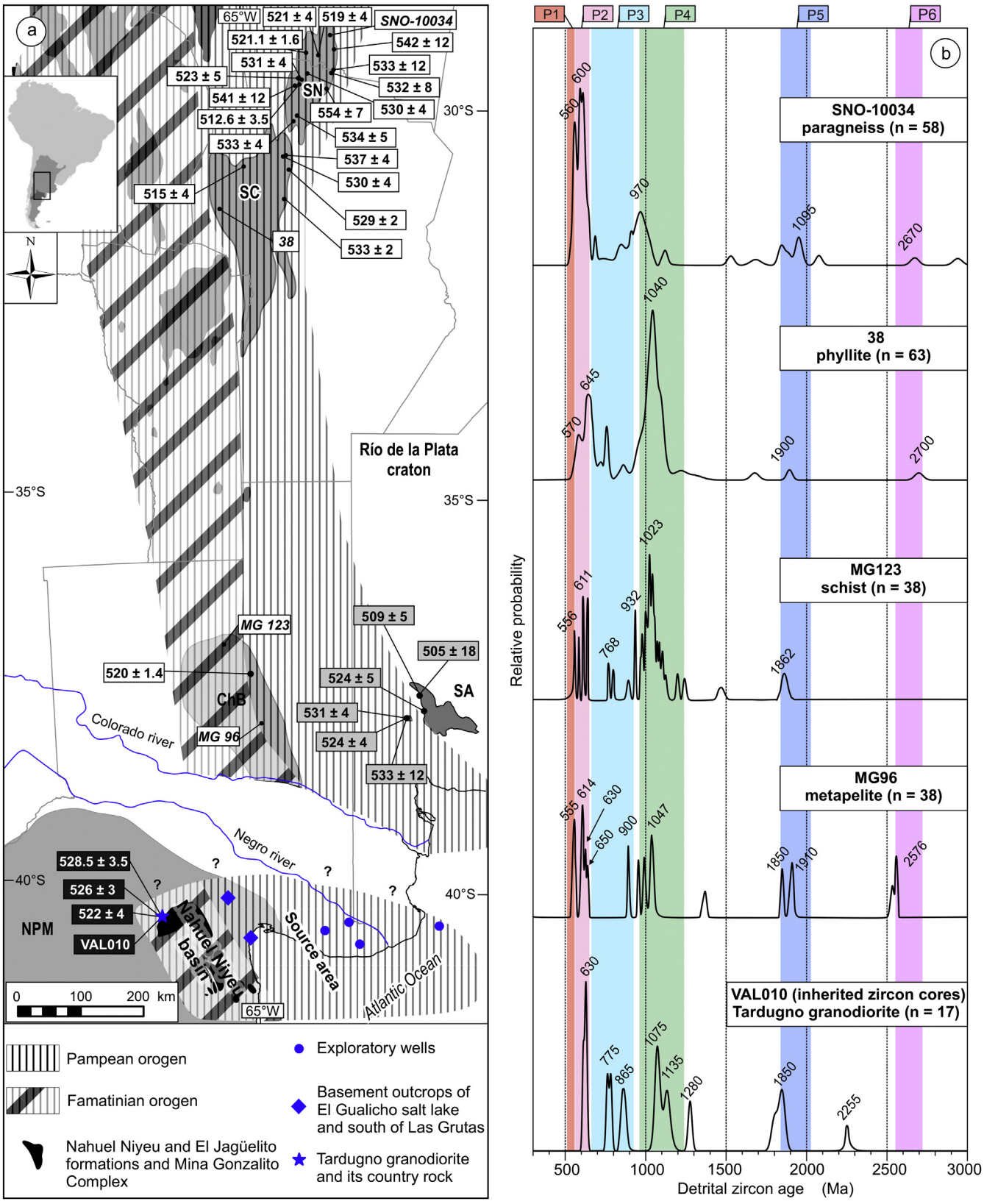

Fig. 15. The Nahuel Niyeu forearc basin in an autochthonous eastern North Patagonian Massif (NPM). (a) Location of the basin and its proximal source area, and situation of the Pampean and Famatinian orogen of central Argentina region and their potential extension southward into northern Patagonia. The proximal source area of the Nahuel Niyeu basin might have been formed by rocks of the Pampean orogen; part of the Pampean rocks might have formed the substratum of the basin (Tardugno granodiorite and its country rock). Dark grey boxes correspond to geochronological data of the Tardugno granodiorite (Rapalini et al., 2013; Pankhurst et al., 2014). The map also shows sample localities of basement rocks of the Pampean orogen comparable with proximal sources of the Nahuel Niyeu basin. White boxes correspond to the Pampean igneous rocks. Samples of Pampean igneous rocks are compiled from the following works: eastern sector of Eastern Sierras Pampeanas (Sierras de Córdoba -SC-, and Sierra Norte de Córdoba and their northern continuation in

connection in the early Paleozoic and relation to the Ross orogen of the Transantarctic Mountains (Naipauer et al., 2010; González et al., 2010, 2011a, 2011b, 2011d; Ramos and Naipauer, 2014). This connection is mainly based on the archeocyath fauna contained in limestone blocks of the El Jagüelito Formation showing general affinities with archaeocyathan assemblages from the Australia–Antarctica paleobiographic province (González et al., 2011b). These affinities together with lithological, stratigraphical, geochronologica and detrital zircon correlations were interpreted as evidences for an allochthonous origin of the early Paleozoic basement rocks of the eastern North Patagonian Massif, derived from the Transantarctic Mountains of Antarctica (Naipauer et al., 2010; González et al., 2010, 2011a, 2011b, 2011d; Ramos and Naipauer, 2014). In an Antarctic–Patagonia connection context, Ramos and Naipauer (2014) proposed a collision of Patagonia and Eastern Antarctica in the middle–late Cambrian as part of the Ross orogeny, indicating that the North Patagonian Massif is the conjugate margin of the Pensacola Mountains of Antarctica. In this proposal, deformation associated with the collision produced a series of peripheral foreland basins where the protoliths of both the El Jagüelito Formation and correlated units of the Pensacola Mountains were deposited in middle–late Cambrian to Early Ordovician. After this collision, Patagonia would have been rifted and drifted from Eastern Antarctica, and then collided to South America during the late Paleozoic (Ramos and Naipauer, 2014).

Other alternative considers the North Patagonian Massif as an autochthonous part of South America, suggesting that the Pampean and Famatinian orogens from central and northern Argentina (South American margin of Gondwana) might stretch southward into the eastern North Patagonian Massif, implying crustal continuity between these regions since at least the early Paleozoic (Varela et al., 1991; Dalla Salda et al., 1992; Rapela and Pankhurst, 2002; Pankhurst et al., 2003, 2006; Gregori et al., 2008; Rapalini et al., 2013). Further studies also proposed this continuity of the orogens by the early Paleozoic, but consider the North Patagonian Massif as a parautochtonous block rifted from South America during the early–middle Paleozoic, opening a small ocean that subsequently was closed in the late Paleozoic (Rapalini et al., 2010; López de Luchi et al., 2010; Martínez Dopico et al., 2011; Pankhurst et al., 2014).

Crustal continuity between northern Patagonia and the South American margin of Gondwana during the early Paleozoic was indicated from geochronological, geochemical and isotopic studies in the Terreneuvian Tardugno granodiorite and Furongian–Middle Ordovician granitoids of the eastern North Patagonian Massif suggesting continuity of the Pampean and Famatinian arcs from central and northern Argentina through northern Patagonia (Varela et al., 1998, 2008, 2011a; Pankhurst et al., 2003, 2006, 2014; González et al., 2008c; Martínez Dopico et al., 2011; Rapalini et al., 2013). This continuity also was interpreted on the basis of similarities in detrital zircon age patterns of the paraderived-metamorphic basement rocks of the eastern North Patagonian Massif with coeval and similar rocks of the Chadileuvú Block and Eastern Sierras Pampeanas (Rapalini et al., 2010, 2013; Martínez Dopico et al., 2011), and similar Sm-Nd parameters in these regions (Martínez Dopico et al., 2011). In addition, geophysical surveys indicate similar gravimetric characteristics south and north of the late Paleozoic potential suture between north Patagonia and Gondwana, interpreting continental crust of Pampean affinity in both sides of it (Kostadinoff et al., 2005; Gregori et al., 2008, 2013). Furthermore, geologic and/or geophysical evidences for mafic-ultramafic rocks that can represent oceanic crust as an ophiolitic belt related to the late Paleozoic potential suture have not been identified (Kostadinoff et al., 2005; Ramos, 2008; Gregori et al., 2008).

Some evidences for the origin of Patagonia are inconclusive and call for some comment. Detrital zircon patterns of the paraderived metamorphic rocks of the eastern North Patagonian Massif are similar to those of comparable units all along the south margin of Gondwana, including the Eastern Sierras Pampeanas, the Chadileuvú Block, and the Transantarctic Mountains (Rapalini et al., 2010, 2013; Naipauer et al., 2010; Martínez Dopico et al., 2011; González et al., 2011a, 2011b, 2011d; Ramos and Naipauer, 2014; and references therein). Thus, these patterns are not diagnostic for the location of a basin along this margin probably because of similar provenance in such regions (Pankhurst et al., 2014). Likewise, the archeocyath fauna from El Jagüelito Formation might also be considered as an evidence of other possible geotectonic situation with respect to South America. This situation supposes an autochthonous position of the eastern North Patagonian Massif, at the western end of the Australia–Antarctica paleobiogeographic province (González et al., 2011b). In this case, this paleobiogeographic province might have stretched up to Patagonia, along the paleo-Pacific margin of Gondwana (González et al., 2011b). Additionally, late Paleozoic deformation and magmatism in the North Patagonian massif can be explained either in terms of an allochthonous, parautochthonous or autochthonous northern Patagonia (see discussion and references in Ramos, 1984, 2008; von Gosen, 2002, 2003; Pankhurst et al., 2006, 2014 Gregori et al., 2008, 2016; Rapalini et al., 2010; López de Luchi et al., 2010; Martínez Dopico et al., 2011). Regarding to paleomagnetic constraints, paleopoles argue for an autochthonous origin of Patagonia, however their uncertainties permit a separation of up to about 1500 km between the North Patagonian Massif and Gondwana in the Devonian to Middle Carboniferous arguing for a parautochtonous origin (Rapalini et al., 2010 and references therein). All these inconclusive evidences demostrate that the origin of Patagonia and its Paleozoic evolution in the southern margin of Gondwana is a matter of further debate.

6.7.1. Evaluating the Nahuel Niyeu basin in an autochthonous eastern North Patagonian Massif

In order to add to the discussion of the origin of Patagonia, we now proceed to evaluate the development of the Nahuel Niyeu basin considering the autochthonous alternative of the eastern North Patagonian Massif. The evaluation is based on the depicted lines of evidence suggesting crustal continuity between these regions during the early Paleozoic. With this purpose, we compare the established proximal sources of this basin with basement rocks of the Pampean orogen cropping out in the eastern sector of the

the Santiago del Estero Province -SN-; Iannizzotto et al., 2013; Leal et al., 2003; Ramos et al., 2015; Rapela et al., 1998; Schwartz et al., 2008; Siegesmund et al., 2010; Stuart-Smith et al., 1999; von Gosen et al., 2014) and Chadileuvú Block (-ChB-; Chernicoff et al., 2012). Sample localities of basement rocks of Sierras Australes (-SA-; light grey boxes; Rapela et al., 2003; Tohver et al., 2012) also are depicted. The Famatinian orogen in northern Patagonia might be represented by regional metamorphism, ductile deformation, and magmatism that affected the Nahuel Niyeu basin at the end of the Cambrian Epoch 2–Middle Ordovician interval. Note the Pampean substratum of the Famatinian orogen. (b) Normalized relative probability plots of detrital zircon ages correspond to paraderived metamorphic rock of the Pampean orogen. Samples include two examples from the eastern sector of Eastern Sierras Pampeanas (-SC- and -SN-; SNO-10034, Iannizzotto et al., 2013; 38, Escayola et al., 2007) and all published data from the Chadileuvú Block (-ChB-; MG123, Zappettini et al., 2010; MG96, Chernicoff et al., 2010). For comparison, one plot corresponds to the inherited zircon cores from the Tardugno Granodiorite (VAL010) represented in Fig. 10. Numbers over the curves are the ages of probability peaks. n = total analyzed grains. Color bars are the same as in Figs. 7, 9 and 10. The map shows the location of these samples. (For interpretation of the references to colour in this figure legend, the reader is referred to the web version of this article.)

Eastern Sierras Pampeanas (Sierras de Córdoba, and Sierra Norte de Córdoba and their northern continuation in the Santiago del Estero Province) and the Chadileuvú Block. Moreover, we incorporate in the evaluation some of the evidences for the allochthonous origin of Patagonia that are inconclusive but that might be interpreted in an autochthonous scenario (e.g. archaeocyaths and detrital zircon patterns), as was previously discussed. The basement rocks of Sierras Australes also are incorporated in the evaluation. Additionally, we add into consideration the early Paleozoic regional metamorphism and ductile deformation affecting the protoliths of the Nahuel Niyeu and El Jagüelito formations and the Mina Gonzalito Complex (the fill of the Nahuel Niyeu basin) and the magmatism associated with these processes.

High and low-grade paraderived metamorphic rocks associated with the Pampean orogen crop out in the Chadileuvú Block and the eastern sector of the Eastern Sierras Pampeanas (Fig. 15a, Sierras de Córdoba and Sierra Norte de Córdoba). Deposition of their protoliths and a subsequent, first regional metamorphic event (Pampean metamorphism) occurred during the latest Ediacaran–Terreneuvian (Tickyj, 1999; Zappetini et al., 2010; Chernicoff et al., 2010; von Gosen et al., 2014; Baldo et al., 2014). This time interval is coeval with the timing of similar processes interpreted in the paraderived metamorphic sources of the Nahuel Niyeu basin (Fig. 11). Moreover, detrital zircon age patterns of these rocks (e.g. Escayola et al., 2007; Iannizzotto et al., 2013) are similar to the distribution of older detrital zircon ages recorded in the paraderived metamorphic rocks of the basement of the eastern North Patagonian Massif (P2 to P6 populations in our samples and corresponding detrital zircon ages reported by other authors, suggested as supplied from the paraderived metamorphic sources). This similarity is evidenced by (cf. Figs. 9 and 15b): (1) youngest probability peak close in age to the limit between the P1 and P2 populations (2) oldest probability peaks temporally equivalent to the ages of the P2 to P6 populations. Furthermore, detrital zircon age patterns of these Pampean metamorphic rocks also are similar to the age distribution of the inherited zircon cores of the Tardugno granodiorite (cf. Figs. 10, 15a and b).

Calc-alkaline, mainly acidic subvolcanic and plutonic rocks of the Pampean arc with SHRIMP and TIMS U–Pb zircon crystallization ages of 554 to ca. 513 Ma intrude the paraderived metamorphic rocks from the eastern sector of the Eastern Sierras Pampeanas (Fig. 15a; von Gosen et al., 2014; Baldo et al., 2014; Ramos et al., 2015). The youngest (530–~513 Ma), calc-alkaline rocks of this arc, particularly those intrusions cropping out in the Sierra Norte de Córdoba and their northern continuation in the Santiago del Estero Province (Fig. 14), were linked to a phase of uplift and extension after cessation of Pampean deformation and regional metamorphism (a post-orogenic extensional stage of the Pampean orogeny) (Leal et al., 2003; von Gosen et al., 2014; Ramos et al., 2015). All these Pampean arc rocks exhibit ages and composition like those of the older (555–>520 Ma) and younger (520–510 Ma) proximal igneous sources of the Nahuel Niyeu basin. Moreover, the paraderived metamorphic and igneous Pampean rocks represent an association of rocks (magmatic arc and country rocks) similar to that interpreted in the proposed source area of the Nahuel Niyeu basin (Fig. 11). A calc-alkaline metadiorite with a SHRIMP U–Pb zircon crystallization age of 520 Ma from the Chadileuvú Block (Fig. 15a) represents a poorly exposed segment of the Pampean magmatic arc (Chernicoff et al., 2012) and is coeval with the younger igneous sources of the Nahuel Niyeu basin.

The above comparisons show that igneous and metamorphic basement rocks related to the Pampean orogen have significant similarities with the proximal source rocks established for the Nahuel Niyeu forearc basin. In addition, the post-orogenic extensional stage of the Pampean orogeny (530–~513 Ma) overlaps in time deposition in the Nahuel Niyeu basin (~520–510 Ma) and is consistent with the extensional tectonic regime associated with the basin. These findings support the continuity of the Pampean orogen from central and northern Argentina southward into northern Patagonia (Fig. 15a; e.g. Varela et al., 1991; Rapela and Pankhurst, 2002; Pankhurst et al., 2003, 2006, 2014; Kostadinoff et al., 2005; Gregori et al., 2008; Rapalini et al., 2013). Considering this possibility, the proximal source area of the Nahuel Niyeu forearc basin might have been constituted by rocks belonging to the Pampean orogen (Fig. 14). This is consistent with gravimetric highs considered as continental crust with Pampean affinity located in this source area (Kostadinoff et al., 2005; Gregori et al., 2008, 2013). Also, part of the Pampean rocks might have formed the substratum of the basin (the Terreneuvian Tardugno granodiorite and its country rock, see discussion in Section 6.6) (Figs. 14 and 15a). Hence, the Nahuel Niyeu basing might have been developed over the paleo-Pacific Ocean side of the possible southern continuation of the Pampean orogen in northern Patagonia, during the end of the post-orogenic extensional stage of the Pampean orogeny (~520–510 Ma, Cambrian Epoch 2) (Fig. 14). This tectonic scenario is consistent with a landward-dipping subduction of the paleo-Pacific Ocean beneath the southwestern margin of Gondwana during the Cambrian (e.g. Curtis, 2001; Cawood, 2005; Cawood and Buchan, 2007; Schwartz et al., 2008; Tohver et al., 2012). In a regional context, the local carbonate platforms of the Nahuel Niyeu basin, interpreted as the source of the archaeocyathan limestone blocks of the El Jagüelito Formation (Section 6.6; Fig. 14), might represent the western end of the Australia–Antarctica palaeobiogeographic province in northern Patagonia (González et al., 2011b). Furthermore, the similar distribution of detrital zircon ages recorded both in the paraderived metamorphic rocks of the basement of the eastern North Patagonian Massif and in the coeval and similar rocks of the Chadileuvú Block and Eastern Sierras Pampeanas might reflect development of coeval basins and similar sources in these regions (Rapalini et al., 2013).

I- and A-type granites and peralkaline rhyolites with crystallization ages of 533–524 Ma and 509–505 Ma (SHRIMP U–Pb zircon ages, Rapela et al., 2003; Tohver et al., 2012), respectively, are part of the basement of the Sierras Australes (Fig. 15a). The peralkaline rhyolites were interpreted as representing a continental rifting event probably started during the intrusion of the I- and A-Type granites (Rapela et al., 2003). However, this extensional-related magmatism is coeval with the Pampean arc and might be considered as developed along the southern margin of the Rio de la Plata craton inboard of the region with active deformation, magmatism and crustal reworking of the Pampean orogen (Tohver et al., 2012). Moreover, the rifting event is coeval with the post-orogenic extensional stage of the Pampean orogeny and both overlap in time deposition in the Nahuel Niyeu forearc basin. Thus, the rifting event in Sierras Australes might have been related to the formation of a marginal basin above an active subduction zone along the South American margin of Gondwana (Cawood and Buchan, 2007). In this tectonic context, the Pampean orogen might have been between the Nahuel Niyeu forearc basin and this marginal basin. This situation also supports the continuation of this orogen toward northern Patagonia and a landward-dipping subduction of the paleo-Pacific Ocean beneath the southwestern margin of Gondwana at the Cambrian.

Regional metamorphism and ductile deformation affecting the protoliths of the Nahuel Niyeu and El Jagüelito formations and the Mina Gonzalito Complex (the fill of the Nahuel Niyeu basin) took place at the end of the Cambrian Epoch 2–Early Ordovician interval (Greco et al., 2015 and references therein). These orogenic processes were accompanied by Furongian to Middle Ordovician magmatism, represented by the granodioritic orthogneiss of the

Mina Gonzalito Complex and the granitoids of the Punta Sierra Plutonic Complex (Greco et al., 2015 and references therein). All these processes might be related to the Famatinian orogeny from central and northern Argentina, suggesting the continuity of the Famatinian orogen southward into northern Patagonia (Fig. 15a; Dalla Salda et al., 1992; Rapela and Pankhurst, 2002; Pankhurst et al., 2003, 2006; Gregori et al., 2008; González et al., 2008c; Rapalini et al., 2010, 2013; Martínez Dopico et al., 2011). Therefore, the Nahuel Niyeu basin (and probably its Pampean substratum, Tardugno granodiorite and its country rock) was subsequently affected by regional metamorphism, ductile deformation, and magmatism that might have been related to the Famatinian orogeny at the end of the Cambrian Epoch 2–Middle Ordovician interval (Fig. 15a). A similar situation occurred in the eastern Sierras Pampeanas where the western boundary of the Pampean orogen was then affected by magmatism, deformation and regional metamorphism of the Famatinian orogeny (Fig. 15a; Sato et al., 2003). Accordingly, the relative position of the Pampean and Famatinian orogens in northern Patagonia seems to be the same that in the eastern Sierras Pampeanas (Fig. 15a), as was earlier proposed by Rapela and Pankhurst (2002).

Overall, our evaluation of the development of the Nahuel Niyeu basin and its subsequent orogenic evolution, in an autochthonous North Patagonian Massif, supports the previous ideas suggesting continuity of the Pampean and Famatinian orogen from Northwestern Argentina and Eastern Sierras Pampeanas regions southward into northern Patagonia. However, as there are still no conclusive evidences for the origin of Patagonia, we suggest this connection as a possibility only.

7. Conclusions

As the result of the study of the metasedimentary rocks of the Nahuel Niyeu Formation at Aguada Cecilio area, we can draw the following conclusions:

(a) Within the Aguada Cecilio area, we have grouped the metasedimentary rocks into three metasedimentary lithofacies according to their lithology and color (greyish green, yellowish brown and red lithofacies).
(b) From detrital zircon studies of metagreywackes, we have obtained maximum depositional ages of the siliciclastic protoliths of the three lithofacies between 516.8 and 516.2 Ma. Combining these ages with the crystallization age of prekinematic sills intercalated in the metasedimentary lithofacies, we have limited the deposition of the siliciclastic protoliths in the Aguada Cecilio area to the Cambrian Epoch 2 between 516.8–516.2 Ma and 513.6 Ma.
(c) From the new ages and the previous data reported by other researchers, we suggest a Cambrian Epoch 2 (~520–510 Ma) deposition of the siliciclastic protoliths of the entire Nahuel Niyeu Formation.
(d) The siliciclastic protoliths of the Nahuel Niyeu Formation were compositionally and texturally immature with provenance from a proximal source area. The most likely source rocks of this area were three: (1) 520–510 Ma, acidic volcanic rocks representing an active magmatic arc, (2) ~555–>520 Ma, acidic plutonic and volcanic rocks representing earlier stages of the same active magmatic arc and (3) low to high-grade, paraderived metamorphic rocks with deposition and regional metamorphism during the latest Ediacaran–Terreneuvian interval, representing the country rocks of the arc.
(e) Our regional comparison throughout the North Patagonian Massif and detrital zircon analysis agrees with an earlier idea of Greco et al. (2015) of consider the siliciclastic and intercalated igneous protoliths of the Nahuel Niyeu and El Jagüelito formations and the Mina Gonzalito Complex as formed in a convergent continental margin basin associated with an active magmatic arc. This basin would have developed during the Cambrian Epoch 2 (~520–510 Ma), receiving detritus mainly from the proximal source area established for the siliciclastic protoliths of the Nahuel Niyeu Formation. We named this basin as “Nahuel Niyeu basin”. Rocks equivalent to the metamorphic and older igneous sources would have been part of the substratum of the basin.
(f) The Nahuel Niyeu basin possibly was elongated in the ~NW–SE direction with the proximal source area located toward its northeastern side (present coordinates). We interpret the basin as a forearc basin associated with an extensional regime.
(g) According to our evaluation, the development of the Nahuel Niyeu forearc basin and its subsequent orogenic evolution seem to be consistent with an autochthonous situation of the eastern North Patagonian Massif.

Acknowledgements

We gratefully acknowledge the assistance provided to us by Guillermo Cecchi and Ricardo Flores to perform our field works. We specially thank for the kindness and hospitality, and laboratory support to Walter Sproesser, Solange de Souza, and Helen and Ivone Sonoki, in our stay in Brasil. We warmly acknowledge the reviews by W. von Gosen and M. Naipauer, which improved greatly the original manuscript. Field and laboratory works was supported by the projects PIP-CONICET 112-201101-00324, PICT-2015-0787 and PI-UNRN-40-A-462.

Appendix A. Supplementary data

Supplementary data related to this article can be found at http://dx.doi.org/10.1016/j.jsames.2017.07.009.

References

Aragón, E., Rodriguez, A.M.I., Benialgo, A., 1996. A calderas field at the Marifil Formation, new volcanogenic interpretation, Norpatagonian Massif, Argentina. J. S. Am. Earth Sci. 9, 321–328. http://dx.doi.org/10.1016/S0895-9811(96)00017-X.
Babcock, L.E., Peng, S., 2007. Cambrian chronostratigraphy: current state and future plans. Palaeogeography, Palaeoclimatology. Palaeoecology 254, 62–66. http://dx.doi.org/10.1016/j.palaeo.2007.03.011.
Baldo, E.G., Rapela, C.W., Pankhurst, R.J., Galindo, C., Casquet, C., Verdecchia, S.O., Murra, J.A., 2014. Geocronología de las Sierras de Córdoba: revisión y comentarios. In: Martino, R.D., Guareschi, A.B. (Eds.), Geología y Recursos Naturales de la provincia de Córdoba. Asociación Geológica Argentina, Córdoba, pp. 845–868.
Basei, M.A.S., Varela, R., Sato, A.M., Siga Jr., O., Llambías, E.J., 2002. Geocronología sobre rocas del Complejo Yaminué, Macizo Norpatagónico, Río Negro, Argentina. In: Cabaleri, N.G., Cingolani, C.A. (Eds.), XV Congreso Geológico Argentino. El Calafate, Actas, pp. 117–122.
Bloomer, S.H., Ewart, A., Hergt, J.M., Bryan, W.B., 1994. Geochemistry and origin of igneous rocks from the outer Tonga forearc (Site 841). Scientific Results. College Station, TX (Ocean Drilling Program). In: Hawkins, J., et al. (Eds.), Proceedings of the Ocean Drilling Program, pp. 625–646. http://dx.doi.org/10.2973/odp.proc.sr.135.129.1994.
Boggs, S.J., 2009. Petrology of Sedimentary Rocks, 2 ed. Cambridge, New York.
Braitsch, O., 1965. Das Paläozoikum von Sierra Grande (Prov. Rio Negro, Argentinien) und die altkaledonische Faltung im östlichen Andenvorland. Geol. Rundsch. 54, 698–714. http://dx.doi.org/10.1007/BF01820752.
Busteros, A., Giacosa, R., Lema, H., 1998. Hoja Geológica 4166-IV, Sierra Grande, Provincia de Río Negro. Servicio Geológico Minero Argentino, Buenos Aires.
Cagnoni, M.C., Linares, E., Ostera, H.A., Parica, C.A., Remesal, M.B., 1993. Caracterización geoquímica de los metasedimentos de la Formación Nahuel Niyeu: implicancias sobre su proveniencia y marco tectónico. In: XII Congreso Geológico Argentino y 2 Congreso de Exploración de Hidrocarburos. Actas, Mendoza, pp. 281–288.
Caminos, R., 1983. Descripción geológica de las Hojas 39g, Cerro Tapiluke y 39h,

Chipauquil, provincia de Río Negro. Servicio Geológico Nacional, Buenos Aires.
Caminos, R., 2001. Hoja Geológica 4166-I, Valcheta, provincia de Río Negro. Instituto de Geología y Recursos Minerales - Servicio Geológico Minero Argentino, Buenos Aires.
Caminos, R., Llambías, E.J., 1984. El Basamento Cristalino. In: Ramos, V.A. (Ed.), Geología y Recursos Naturales de la Provincia de Río Negro. IX Congreso Geológico Argentino, Buenos Aires, pp. 37–63.
Cawood, P.A., 2005. Terra Australis orogen: rodinia breakup and development of the Pacific and Iapetus margins of Gondwana during the neoproterozoic and Paleozoic. Earth-Science Rev. 69, 249–279. http://dx.doi.org/10.1016/j.earscirev.2004.09.001.
Cawood, P.A., Buchan, C., 2007. Linking accretionary orogenesis with supercontinent assembly. Earth-Science Rev. 82, 217–256. http://dx.doi.org/10.1016/j.earscirev.2007.03.003.
Cawood, P.A., Hawkesworth, C.J., Dhuime, B., 2012. Detrital zircon record and tectonic setting. Geology 40, 875–878. http://dx.doi.org/10.1130/g32945.1.
Chernicoff, C.J., Caminos, R., 1996a. Estructura y relaciones estratigráficas de la Formación Nahuel Niyeu, Macizo Nordpatagónico oriental, Provincia de Río Negro. Rev. la Asoc. Geol. Argent. 51, 201–212.
Chernicoff, C.J., Caminos, R., 1996b. Estructura y metamorfismo del Complejo Yaminué, Macizo Nordpatagónico oriental, provincia de Río Negro. Rev. la Asoc. Geol. Argent. 51, 107–118.
Chernicoff, C.J., Zappettini, E.O., Santos, J.O.S., Belousova, E., McNaughton, N.J., 2010. SHRIMP U–Pb ages and Hf isotope composition of Las Piedras formation (Ediacaran–Lower Cambrian), southern La Pampa Province, Argentina. In: 7th South American Symposium on Isotope Geology. Brasilia (Abstracts in CD).
Chernicoff, C.J., Zappettini, E.O., Santos, J.O.S., Godeas, M.C., Belousova, E., McNaughton, N.J., 2012. Identification and isotopic studies of early Cambrian magmatism (El Carancho Igneous Complex) at the boundary between Pampia terrane and the Río de la Plata craton, La Pampa province, Argentina. Gondwana Res. 21, 378–393. http://dx.doi.org/10.1016/j.gr.2011.04.007.
Chernicoff, C.J., Zappettini, E.O., Santos, J.O.S., McNaughton, N.J., Belousova, E., 2013. Combined U-Pb SHRIMP and Hf isotope study of the Late Paleozoic Yaminué Complex, Rio Negro Province, Argentina: implications for the origin and evolution of the Patagonia composite terrane. Geosci. Front. 4, 37–56. http://dx.doi.org/10.1016/j.gsf.2012.06.003.
Cortés, J., 1981. El substrato precretácico del extremo noreste de la Provincia del Chubut. Rev. la Asoc. Geol. Argent. 36, 217–235.
Curtis, M.L., 2001. Tectonic history of the Ellsworth Mountains, West Antarctica: reconciling a Gondwana enigma. Geol. Soc. Am. Bull. 113, 939–958 http://dx.doi.org/10.1130/0016-7606(2001)113<0939:thotem>2.0.co;2.
Dalla Salda, L.H., Cingolani, C.A., Varela, R., 1992. Early Paleozoic orogenic belt of the Andes in southwestern South America: result of Laurentia-Gondwana collision? Geology 20, 617–620 http://dx.doi.org/10.1130/0091-7613(1992)020<0617:epobot>2.3.co;2.
Dalla Salda, L.H., Aragón, E., Benialgo, A., Abre, P., Pezzotti, C., 2003a. El protolito siliciclástico de las Ectinitas El Jagüelito, provincia de Río Negro. Rev. la Asoc. Geol. Argent. 58, 321–328.
Dalla Salda, L.H., Aragón, E., Benialgo, A., Pezzotti, C., 2003b. Una plataforma calcárea en el Complejo Mina Gonzalito, provincia de Río Negro. Rev. la Asoc. Geol. Argent. 58, 209–217.
de Alba, E., 1964. Descripción Geológica de la hoja 41j Sierra Grande. Dirección Nacional de Geología y Minería, Buenos Aires.
Dickinson, W.R., 1995. Forearc Basins. In: Busby, C.J., Ingersoll, R.V. (Eds.), Tectonics of Sedimentary Basins. Blackwell Science, Oxford, pp. 221–261.
Dickinson, W.R., Seely, D.R., 1979. Structure and stratigraphy of forearc regions. Am. Assoc. Pet. Geol. Bull. 63, 2–31.
Martínez Dopico, C.I., Tohver, E., López de Luchi, M.G., Wemmer, K., Rapalini, A.E., Cawood, P.A., 2016. Jurassic cooling ages in Paleozoic to early Mesozoic granitoids of northeastern Patagonia: 40Ar/39Ar, 40K–40Ar mica and U–Pb zircon evidence. Int. J. Earth Sci. 1–15. http://dx.doi.org/10.1007/s00531-016-1430-0.
Dorobek, S.L., 2008. Carbonate-platform facies in volcanic-arc settings: Characteristics and controls on deposition and stratigraphic development. Geol. Soc. Am. Special Pap. 436, 55–90. http://dx.doi.org/10.1130/2008.2436(04).
Escayola, M.P., Pimentel, M.M., Armstrong, R., 2007. Neoproterozoic backarc basin: Sensitive high-resolution ion microprobe U-Pb and Sm-Nd isotopic evidence from the Eastern Pampean Ranges, Argentina. Geology 35, 495–498. http://dx.doi.org/10.1130/g23549a.1.
Folk, R.L., 1951. Stages of textural maturity in sedimentary rocks. J. Sediment. Res. 21.
Forsythe, R., 1982. The late Palaeozoic to early Mesozoic evolution of southern South America: a plate tectonic interpretation. J. Geol. Soc. 139, 671–682. http://dx.doi.org/10.1144/gsjgs.139.6.0671.
García, V.A., González, S.N., Tassinari, C.C.G., Sato, K., Sato, A.M., González, P.D., Varela, R., 2014a. U/Pb and Nd data from Peñas Blancas Pluton, North Patagonian Massif, Argentina. In: 9th South American Symposium on Isotope Geology. São Paulo. Abstracts, 190.
García, V.A., González, S.N., Tassinari, C.C.G., Sato, K., Sato, A.M., González, P.D., Varela, R., 2014b. Geoquímica y geocronología del Plutón La Verde, Macizo Nordpatagónico, provincia de Río Negro. In: Martino, R.D., et al. (Eds.), XIX Congreso Geológico Argentino. Córdoba, Actas, pp. 373–374.
Gärtner, A., Linnemann, U., Sagawe, A., Hofmann, M., Ullrich, B., Kleber, A., 2013. Morphology of zircon crystal grains in sediments—characteristics, classifications, definitions. Geol. Saxonica 59, 65–73.
Giacosa, R., 1987. Caracterización de un sector del basamento metamórfico-migmatítico en el extremo suroriental del Macizo Norpatagónico, Provincia de Río Negro, Argentina. In: X Congreso Geológico Argentino. San Miguel de Tucumán, Actas, pp. 51–54.
Giacosa, R., 1997. Geología y petrología de las rocas pre-cretácicas de la región de Sierra Pailemán, Provincia de Río Negro. Rev. la Asoc. Geol. Argent. 52, 65–80.
Giacosa, R., 1999. El basamento pre-silúrico del extremo este del Macizo Nordpatagónico y del Macizo del Deseado. In: Caminos, R. (Ed.), Geología Argentina. Instituto de Geología y Recursos Minerales – SEGEMAR, Buenos Aires, pp. 118–123.
Giacosa, R., 2001. Zonas de cizalla frágil-dúctil neopaleozoicas en el nordeste de la Patagonia. Rev. la Asoc. Geol. Argent. 56, 131–140.
Giacosa, R., Paredes, J., 2001. Estructura de las metamorfitas del Paleozoico temprano en el Arroyo. Salado. Macizo Nordpatagónico, Río Negro. Rev. la Asoc. Geol. Argent. 56, 141–149.
González, P.D., Poiré, D., Varela, R., 2002. Hallazgo de trazas fósiles en la Formación El Jagüelito y su relación con la edad de las metasedimentitas, Macizo Nordpatagónico Oriental, provincia de Río Negro. Rev. la Asoc. Geol. Argent. 57, 35–44.
González, P.D., Varela, R., Sato, A.M., Llambías, E.J., González, S.N., 2008a. Dos fajas estructurales distintas en el Complejo Mina Gonzalito, Río Negro. In: XVII Congreso Geológico Argentino. San Salvador de Jujuy, Actas, pp. 847–848.
González, P.D., Varela, R., Sato, A.M., Campos, H., Greco, G.A., Naipauer, M., Llambías, E.J., García, V., 2008b. Metamorfismo regional Ordovícico y estructura de la Ectinita El Jagüelito al SO de Sierra Grande, Río Negro. In: XVII Congreso Geológico Argentino. San Salvador de Jujuy, Actas, pp. 849–850.
González, P.D., Sato, A.M., Varela, R., Llambías, E.J., Naipauer, M., Basei, M., Campos, H., Greco, G.A., 2008c. El Molino Plutón: a granite with regional metamorphism within El Jagüelito formation, North Patagonian Massif. In: Linares, E., et al. (Eds.), 6th South American Symposium on Isotope Geology. San Carlos de Bariloche. Volume en CD, Paper Nº 41.
González, P.D., Varela, R., Sato, A.M., Greco, G.A., Naipauer, M., Llambías, E., 2010. Evidencias geológicas y paleontológicas en la Formación El Jagüelito para la conexión Patagonia-Antártida durante el Paleozoico inferior. In: X Congreso Argentino de Paleontología y Bioestratigrafía y VII Congreso Latinoamericano de Paleontología. La Plata, Actas en CD, vol. 48.
González, P.D., Sato, A.M., Varela, R., Llambías, E.J., Greco, G.A., González, S.N., García, V., 2011a. Conexión Macizo Norpatagónico - Antártida Oriental: fósiles Arqueociátidos, comparación geológica y circones detríticos. In: Leanza, H., et al. (Eds.), XVIII Congreso Geológico Argentino. Neuquén, Actas en CD, pp. 87–88.
González, P.D., Tortello, M.F., Damborenea, S.E., 2011b. Early cambrian archaeocyathan limestone blocks in low-grade meta-conglomerate from el jagueelito formation (Sierra Grande, Río Negro, Argentina). Geol. Acta 9, 159–173.
González, P.D., Greco, G.A., Varela, R., Naipauer, M., Sato, A.M., Llambías, E.J., García, V., Campos, H., 2011c. Patrón metamórfico invertido en la Formación El Jagüelito de la Herradura del Salado, Basamento Norpatagónico, Río Negro. In: Leanza, H., et al. (Eds.), XVIII Congreso Geológico Argentino. Neuquén, Actas en CD, pp. 85–86.
González, P.D., Sato, A.M., Naipauer, M., Varela, R., Llambías, E., Basei, M.A.S., Sato, K., Sproesser, W., 2011d. Does Patagonia represent a missing piece detached from the Ross Orogen. In: Schmitt, R.S., et al. (Eds.), Gondwana 14. Rio de Janeiro, Brasil, Abstracts, 153.
González, P.D., Sato, A.M., Varela, R., Naipauer, M., Llambías, E.J., Castro Dorado, A., 2013. Volcanismo de arco asociado a la Formación El Jagüelito, Sierra Grande, Río Negro. In: 2º Simposio Petrología Ígnea y Metalogénesis Asociada. San Luis, Libro de actas, pp. 39–40.
González, P.D., Sato, A.M., Varela, R., Greco, G.A., Naipauer, M., Llambías, E.J., Basei, M.A.S., 2014a. Metamorfismo y estructura interna de la Formación El Jagüelito en el Arroyo Salado inferior, Macizo Norpatagónico, Río Negro. In: Martino, R.D., et al. (Eds.), XIX Congreso Geológico Argentino. Córdoba, Actas en CD, pp. 381–382.
González, S.N., Greco, G.A., González, P.D., Sato, A.M., Llambías, E.J., Varela, R., Basei, M.A.S., 2014b. Geología, petrografía y edad U-Pb de un enjambre longitudinal NO-SE de diques del macizo nordpatagónico oriental, Río negro. Rev. la Asoc. Geol. Argent. 71, 174–183.
González, S.N., Greco, G.A., González, P.D., Sato, A.M., Llambías, E.J., Varela, R., 2016. Geochemistry of a Triassic dyke swarm in the North Patagonian Massif, Argentina. Implications for a postorogenic event of the Permian Gondwanide orogeny. J. S. Am. Earth Sci. 70, 69–82. http://dx.doi.org/10.1016/j.jsames.2016.04.009.
González, S.N., Greco, G.A., Sato, A.M., Llambías, E.J., Basei, M.A.S., González, P.D., Díaz, P.E., 2017. Middle Triassic trachytic lava flows associated with coeval dyke swarm in the North Patagonian Massif: a postorogenic magmatism related to extensional collapse of the Gondwanide orogen. J. S. Am. Earth Sci. 75, 134–143. http://dx.doi.org/10.1016/j.jsames.2017.02.007.
Gozalvez, M.R., 2009a. Caracterización del plutón San Martín y las mineralizaciones de wolframio asociadas, departamento Valcheta, provincia de Río Negro. Rev. la Asoc. Geol. Argent. 64, 409–425.
Gozalvez, M.R., 2009b. Petrografía y edad 40Ar/39Ar de leucogranitos peraluminosos al oeste de Valcheta: Macizo Nordpatagónico (Río Negro). Rev. la Asoc. Geol. Argent. 64, 285–294.
Greco, G.A., González, S.N., Sato, A.M., González, P.D., Llambías, E.J., Basei, M.A.S., 2014. Nueva datación en circones detríticos para el Complejo Mina Gonzalito, Provincia de Río Negro. In: Martino, R.D., et al. (Eds.), XIX Congreso Geológico Argentino. Córdoba, Actas en CD, pp. 1454–1455.
Greco, G.A., González, P.D., González, S.N., Sato, A.M., Basei, M.A.S., Tassinari, C.C.G.,

Sato, K., Varela, R., Llambías, E.J., 2015. Geology, structure and age of the Nahuel Niyeu Formation in the Aguada Cecilio area, North Patagonian Massif, Argentina. J. S. Am. Earth Sci. 62, 12–32. http://dx.doi.org/10.1016/j.jsames.2015.04.005.

Gregori, D.A., Kostadinoff, J., Strazzere, L., Raniolo, A., 2008. Tectonic significance and consequences of the Gondwanide orogeny in northern Patagonia, Argentina. Gondwana Res. 14, 429–450. http://dx.doi.org/10.1016/j.gr.2008.04.005.

Gregori, D.A., Kostadinoff, J., Alvarez, G., Raniolo, A., Strazzere, L., Martínez, J.C., Barros, M., 2013. Preandean geological configuration of the eastern North Patagonian Massif, Argentina. Geosci. Front. 4, 693–708. http://dx.doi.org/10.1016/j.gsf.2013.01.001.

Gregori, D.A., Saini-Eidukat, B., Benedini, L., Strazzere, L., Barros, M., Kostadinoff, J., 2016. The Gondwana orogeny in northern North Patagonian Massif: evidences from the caita có granite, La Seña and Pangaré mylonites, Argentina. Geosci. Front. 7, 621–638. http://dx.doi.org/10.1016/j.gsf.2015.06.002.

Hervé, F., Haller, M., Duhart, P., Fanning, C.M., 2005. SHRIMP U–Pb ages of detrital zircons from cushamen and esquel formations, North Patagonian Massif, Argentina: geological implications. In: XVI Congreso Geológico Argentino. La Plata, Actas, pp. 309–314.

Hervé, F., Calderon, M., Fanning, C.M., Pankhurst, R.J., Fuentes, F., Rapela, C.W., Correa, J., Quezada, P., Marambio, C., 2016. Devonian magmatism in the accretionary complex of southern Chile. J. Geol. Soc. http://dx.doi.org/10.1144/jgs2015-163.

Iannizzotto, N.F., Rapela, C.W., Baldo, E.G.A., Galindo, C., Fanning, C.M., Pankhurst, R.J., 2013. The Sierra Norte-Ambargasta batholith: Late Ediacaran–early Cambrian magmatism associated with Pampean transpressional tectonics. J. S. Am. Earth Sci. 42, 127–143. http://dx.doi.org/10.1016/j.jsames.2012.07.009.

Jerram, D.A., 2001. Visual comparators for degree of grain-size sorting in two and three-dimensions. Comput. Geosci. 27, 485–492. https://doi.org/10.1016/S0098-3004(00)00077-7.

Jordan, T.E., 1995. Retroarc foreland and related Basins. In: Busby, C.J., Ingersoll, R.V. (Eds.), Tectonics of Sedimentary Basins. Blackwell Science, Oxford, pp. 331–362.

Kaasschieter, J.P.H., 1965. Geología de la Cuenca del Colorado. In: 2º Jornadas Geológicas Argentinas. Tucumán, pp. 251–271.

Kostadinoff, J., Gregori, D.A., Raniolo, A., 2005. Configuración geofísica-geológica del sector norte de la provincia de Río Negro. Rev. la Asoc. Geol. Argent. 60, 368–376.

Leal, P.R., Hartmann, L.A., Santos, J.O.S., Miró, R.C., Ramos, V.A., 2003. Volcanismo postorogénico en el extremo norte de las Sierras Pampeanas Orientales: Nuevos datos geocronológicos y sus implicancias tectónicas. Rev. la Asoc. Geol. Argent. 58, 593–607.

López de Luchi, M.G., Wemmer, K., Rapalini, A.E., 2008. The cooling history of the North Patagonian Massif: first results for the granitoids of the Valcheta area, Río Negro, Argentina. In: Linares, E., et al. (Eds.), 6th South American Symposium on Isotope Geology. San Carlos de Bariloche. Abstracts, 33.

López de Luchi, M.G., Rapalini, A.E., Tomezzoli, R.N., 2010. Magnetic fabric and microstructures of Late Paleozoic granitoids from the North Patagonian Massif: Evidence of a collision between Patagonia and Gondwana? Tectonophysics 494, 118–137. http://dx.doi.org/10.1016/j.tecto.2010.09.003.

Malvicini, L., Llambías, E., 1974. Geología y génesis del depósito de manganeso Arroyo Verde, provincia del Chubut. In: V Congreso Geológico Argentino. Córdoba, Actas, pp. 185–202.

Marlow, M.S., Johnson, L.E., Pearce, J.A., Fryer, P.B., Pickthorn, L.B.G., Murton, B.J., 1992a. Upper cenozoic volcanic rocks in the Mariana forearc recovered from drilling at ocean drilling program site 781: implications for forearc magmatism. J. Geophys. Res. Solid Earth 97, 15085–15097. http://dx.doi.org/10.1029/92JB01079.

Marlow, M.S., Johnson, L.E., Pearce, J.A., Fryer, P.B., Pickthorn, L.B.G., Murton, B.J., 1992b. Pleistocene volcanic rocks in the Mariana forearc revealed by drilling at Site 781. In: Fryer, P., et al. (Eds.), Proceedings of the Ocean Drilling Program, pp. 293–310. Scientific Results. College Station, TX (Ocean Drilling Program). http://dx.doi.org/10.2973/odp.proc.sr.125.501.1992.

Márquez, M.J., Massaferro, G.I., Fernández, M.I., Menegatti, N., Navarrete, C.R., 2011. El centro volcánico Sierra Grande: caracterización petrográfica y geoquímica del magmatismo extensional liásico, noroeste de la Patagonia. Rev. la Asoc. Geol. Argent. 68, 555–570.

Marsaglia, K.M., 1995. Interarc and Backarc Basins. In: Busby, C.J., Ingersoll, R.V. (Eds.), Tectonics of Sedimentary Basins. Blackwell Science, Oxford, pp. 299–329.

Martínez Dopico, C.I., López de Luchi, M.G., Rapalini, A.E., Kleinhanns, I.C., 2011. Crustal segments in the North Patagonian Massif, Patagonia: an integrated perspective based on Sm–Nd isotope systematics. J. S. Am. Earth Sci. 31, 324–341. http://dx.doi.org/10.1016/j.jsames.2010.07.009.

Martínez, H., Náñez, C., Lizuain, C.D.M., Turel, A., 2001. Hoja Geológica 4166-II, San Antonio Oeste, provincia de Río Negro. Instituto de Geología y Recursos Minerales - Servicio Geológico Minero Argentino, Buenos Aires.

Naipauer, M., Sato, A.M., González, P.D., Chemale Jr., F., Varela, R., Llambías, E.J., Greco, G.A., Dantas, E., 2010. Eopaleozoic Patagonia-East Antartica connection: fossil and U-Pb evidence from El Jagüelito formation. In: 7th South American Symposium on Isotope Geology. Brasilia, pp. 602–605. Short Paper Volume.

Núñez, E., Bachmann, E.W., de, R.I., Britos, A., Franchi, M., Lizuaín, A., Sepúlveda, E., 1975. Rasgos geológicos del sector oriental del Macizo Somuncura, provincia de Río Negro, República Argentina. In: 2º Congreso Iberoamericano de Geología Económica. Buenos Aires, Actas, pp. 247–266.

Pángaro, F., Ramos, V.A., 2012. Paleozoic crustal blocks of onshore and offshore central Argentina: New pieces of the southwestern Gondwana collage and their role in the accretion of Patagonia and the evolution of Mesozoic south Atlantic sedimentary basins. Mar. Pet. Geol. 37, 162–183. http://dx.doi.org/10.1016/j.marpetgeo.2012.05.010.

Pankhurst, R.J., Rapela, C.W., 1995. Production of Jurassic rhyolite by anatexis of the lower crust of Patagonia. Earth Planet. Sci. Lett. 134, 23–36. http://dx.doi.org/10.1016/0012-821X(95)00103-J.

Pankhurst, R.J., Rapela, C.W., Caminos, R., 1993. Problemas geocronológicos de los granitoides gondwánicos de Nahuel Niyeu, Macizo Norpatagónico. In: XII Congreso Geológico Argentino y Segundo Congreso de Exploración de hidrocarburos. Mendoza, Actas, pp. 99–114.

Pankhurst, R.J., Leat, P.T., Sruoga, P., Rapela, C.W., Márquez, M., Storey, B.C., Riley, T.R., 1998. The Chon Aike province of Patagonia and related rocks in West Antarctica: a silicic large igneous province. J. Volcanol. Geotherm. Res. 81, 113–136. http://dx.doi.org/10.1016/S0377-0273(97)00070-X.

Pankhurst, R.J., Rapela, C.W., Loske, W.P., Márquez, M., Fanning, C.M., 2003. Chronological study of the pre-Permian basement rocks of southern Patagonia. J. S. Am. Earth Sci. 16, 27–44. http://dx.doi.org/10.1016/S0895-9811(03)00017-8.

Pankhurst, R.J., Rapela, C.W., Fanning, C.M., Márquez, M., 2006. Gondwanide continental collision and the origin of Patagonia. Earth-Science Rev. 76, 235–257. http://dx.doi.org/10.1016/j.earscirev.2006.02.001.

Pankhurst, R.J., Rapela, C.W., López De Luchi, M.G., Rapalini, A.E., Fanning, C.M., Galindo, C., 2014. The Gondwana connections of northern Patagonia. J. Geol. Soc. 171, 313–328. http://dx.doi.org/10.1144/jgs2013-081.

Peng, S., Babcock, L.E., Cooper, R.A., 2012. Chapter 19-The Cambrian Period. In: Gradstein, F.M., et al. (Eds.), The Geologic Time Scale. Elsevier, Boston, pp. 437–488. http://dx.doi.org/10.1016/B978-0-444-59425-9.00019-6.

Pettijohn, F.J., Potter, P.E., Siever, R., 1987. Sand and Sandstone. Springer-Verlag, New York.

Ramos, V.A., 1975. Geología del sector oriental del Macizo Nordpatagónico entre Aguada Capitán y la Mina Gonzalito, provincia de Río Negro. Rev. la Asoc. Geol. Argent. 30, 274–285.

Ramos, V.A., 1984. Patagonia: un continente paleozoico a la deriva. In: IX Congreso Geológico Argentino San Carlos de Bariloche, Actas, pp. 311–325.

Ramos, V.A., 2008. Patagonia: a paleozoic continent adrift? J. S. Am. Earth Sci. 26, 235–251. http://dx.doi.org/10.1016/j.jsames.2008.06.002.

Ramos, V.A., Cortés, J.M., 1984. Estructura e interpretación Tectónica. In: Ramos, V.A. (Ed.), IX Congreso Geológico Argentino. Geología y Recursos Naturales de la provincia de Río Negro, pp. 317–346.

Ramos, V.A., Naipauer, M., 2014. Patagonia: where does it come from? J. Iber. Geol. 40. http://dx.doi.org/10.5209/rev_JIGE.2014.v40.n2.45304.

Ramos, V.A., Escayola, M., Leal, P.R., Pimentel, M.M., Santos, J.O.S., 2015. The late stages of the Pampean Orogeny, Córdoba (Argentina): evidence of postcollisional Early Cambrian slab break-off magmatism. J. S. Am. Earth Sci. 64 (Part 2), 351–364. http://dx.doi.org/10.1016/j.jsames.2015.08.002.

Rapalini, A.E., Lopez de Luchi, M.G., Martínez Dopico, C., Lince Klinger, F., Giménez, M., Martínez, P., 2010. Did Patagonia collide against Gondwana in the Late Paleozoic? Some insights from a multidisciplinary study of magmatic units of the North Patagonian Massif. Geol. Acta 8, 349–371. http://dx.doi.org/10.1344/105.000001577.

Rapalini, A.E., López de Luchi, M., Tohver, E., Cawood, P.A., 2013. The South American ancestry of the North Patagonian Massif: geochronological evidence for an autochthonous origin? Terra nova.. 25, 337–342. http://dx.doi.org/10.1111/ter.12043.

Rapela, C.W., Pankhurst, R.J., 2002. Eventos tecto-magmáticos del Paleozoico inferior en el margen proto-Atlántico del sur de Sudamérica. In: Cabaleri, N.G., Cingolani, C.A. (Eds.), XV Congreso Geológico Argentino. El Calafate, Actas, pp. 24–29.

Rapela, C.W., Pankhurst, R.J., Casquet, C., Baldo, E., Saavedra, J., Galindo, C., Fanning, C.M., 1998. The Pampean Orogeny of the southern proto-Andes: Cambrian continental collision in the Sierras de Córdoba. Geol. Soc. Lond., Special Publications 142, 181–217. http://dx.doi.org/10.1144/gsl.sp.1998.142.01.10.

Rapela, C.W., Pankhurst, R.J., Fanning, C.M., Grecco, L.E., 2003. Basement evolution of the Sierra de la Ventana Fold Belt: new evidence for Cambrian continental rifting along the southern margin of Gondwana. J. Geol. Soc. 160, 613–628. http://dx.doi.org/10.1144/0016-764902-112.

Sánchez Lorda, M.E., Sarrionandia, F., Ábalos, B., Carrracedo, M., Eguíluz, L., Gil Ibarguchi, J.I., 2014. Geochemistry and paleotectonic setting of Ediacaran metabasites from the Ossa-Morena Zone (SW Iberia). Int. J. Earth Sci. 103, 1263–1286. http://dx.doi.org/10.1007/s00531-013-0937-x.

Sato, A.M., Tickyj, H., Llambías, E.J., 1998. El basamento ígneometamórfico del área de Las Grutas, provincia de Río Negro, Argentina. In: 10° Congreso Latinoamericano de Geología y 6° Congreso Nacional de Geología Económica., Buenos Aires, Actas, pp. 65–70.

Sato, A.M., González, P.D., Llambías, E.J., 2003. Evolución del orógeno Famatiniano en la Sierra de San Luis: magmatismo de arco, deformación y metamorfismo de bajo a alto grado. Rev. Asoc. Geol. Argent. 54.

Schwartz, J.J., Gromet, L.P., Miró, R., 2008. Timing and duration of the Calc-alkaline arc of the Pampean orogeny: implications for the Late neoproterozoic to Cambrian evolution of Western Gondwana. J. Geol. 116, 39–61. http://dx.doi.org/10.1086/524122.

Serra-Varela, S., Giacosa, R., González, P., Heredia, N., Martín-González, F., Pedreira, D., 2016. Geología y geocronología del basamento paleozoico de los

Andes Norpatagónicos en el área de San Martín de los Andes. GEO-TEMAS 16, 431–434.
Siegesmund, S., Steenken, A., Martino, R.D., Wemmer, K., López de Luchi, M.G., Frei, R., Presnyakov, S., Guereschi, A., 2010. Time constraints on the tectonic evolution of the Eastern Sierras Pampeanas (Central Argentina). Int. J. Earth Sci. 99, 1199–1226. http://dx.doi.org/10.1007/s00531-009-0471-z.
Smith, G.A., Landis, C.A., 1995. Intra-Arc Basins. In: Busby, C.J., Ingersoll, R.V. (Eds.), Tectonics of Sedimentary Basins. Blackwell Science, Oxford, pp. 263–298.
Stuart-Smith, P.G., Camacho, A., Sims, J.P., Skirrow, R.G., Lyons, P., Pieters, P.E., Black, L.P., Miró, R., 1999. Uranium-lead dating of felsic magmatic cycles in the southern Sierras Pampeanas, Argentina: implications for the tectonic development of the proto-Andean Gondwana margin. Geol. Soc. Am. Special Pap. 336, 87–114. http://dx.doi.org/10.1130/0-8137-2336-1.87.
Taylor, R.N., Marlow, M.S., Johnson, L.E., Taylor, B., Bloomer, S.H., Mitchell, J.G., 1995. Intrusive volcanic rocks in Western Pacific forearcs. In: Taylor, B., Natland, J. (Eds.), Active Margins and Marginal Basins of the Western Pacific. American Geophysical Union, Washington, D.C, pp. 31–43. http://dx.doi.org/10.1029/GM088p0031.
Tickyj, H., 1999. Estructura y petrología del basamento cristalino de la porción centro-sur de la provincia de La Pampa, vol. 228. Universidad Nacional de La Plata, Argentina.
Tohver, E., Cawood, P.A., Rossello, E.A., Jourdan, F., 2012. Closure of the Clymene Ocean and formation of West Gondwana in the Cambrian: evidence from the Sierras Australes of the southernmost Rio de la Plata craton, Argentina. Gondwana Res. 21, 394–405. http://dx.doi.org/10.1016/j.gr.2011.04.001.
Trop, J.M., Ridgway, K.D., Spell, T.L., 2003. Sedimentary record of transpressional tectonics and ridge subduction in the Tertiary Matanuska Valley-Talkeetna Mountains forearc basin, southern Alaska. In: Sisson, V.B., et al. (Eds.), Geology of a Transpressional Orogen Developed during Ridge-trench Interaction along the North Pacific Margin. Geological Society of America.
Tucker, M.E., 2001. Sedimentary Petrology: an Introduction to the Origin of Sedimentary Rocks, 3 ed. Wiley-Blackwell.
Underwood, M.B., Moore, G.F., 1995. Trenches and trench-slope Basins. In: Busby, C.J., Ingersoll, R.V. (Eds.), Tectonics of Sedimentary Basins. Blackwell Science, Oxford, pp. 179–219.
Varela, R., Dalla Salda, L., Cingolani, C.A., Gomez, V., 1991. Estructura, petrología y geocronología del basamento de la región del Limay, provincias de Río Negro y Neuquen, Argentina. Rev. Geol. Chile 18, 147–163. http://dx.doi.org/10.5027/andgeoV18n2-a05.
Varela, R., Cingolani, C.A., Sato, A.M., Dalla Salda, L., Brito Neves, B.B., Basei, M.A.S., Siga Jr., O., Teixeira, W., 1997. Proterozoic and paleozoic evolution of Atlantic area of North-Patagonian Massif, Argentine. In: 1st South American symposium on isotope geology. Campos do Jordao, Brasil, pp. 326–329. Extended abstracts.
Varela, R., Basei, M.A.S., Sato, A.M., Siga Jr., O., Cingolani, C.A., Sato, K., 1998. Edades isotópicas Rb/Sr y U/Pb en rocas de Mina Gonzalito y Arroyo Salado. Macizo Norpatagónico Atlántico, Río Negro, Argentina. In: X Congreso Latinoamericano de Geología y VI Congreso Nacional de Geología Económica. Buenos Aires, Actas, pp. 71–76.
Varela, R., Basei, M.A.S., Cingolani, C.A., Siga Jr., O., Passarelli, C.R., 2005. El basamento cristalino de los Andes norpatagónicos en Argentina: geocronología e interpretación tectónica. Rev. Geol. Chile 32, 167–187.
Varela, R., Basei, M.A.S., González, P.D., Sato, A.M., Sato, K., 2008. Granitoides Famatinianos y Gondwánicos en Sierra Grande. Nuevas edades radimétricas método U-Pb. In: XVII Congreso Geológico Argentino. San Salvador de Jujuy, Actas, pp. 914–915.
Varela, R., González, P.D., Basei, M.A.S., Sato, K., Sato, A.M., Naipauer, M., García, V.A., González, S.N., Greco, G.A., 2011a. Edad del Complejo Mina Gonzalito: revisión y nuevos datos. In: Leanza, H., et al. (Eds.), XVIII Congreso Geológico Argentino. Neuquén, Actas en CD, pp. 127–128.
Varela, R., Basei, M.A.S., González, P.D., Sato, A.M., Naipauer, M., Campos Neto, M., Cingolani, C.A., Meira, V.T., 2011b. Accretion of Grenvillian terranes to the southwestern border of the Río de la Plata craton, western Argentina. Int. J. Earth Sci. 100, 243–272. http://dx.doi.org/10.1007/s00531-010-0614-2.
Varela, R., González, P.D., Philipp, R., Sato, A.M., González, S.N., Greco, G.A., Naipauer, M., 2014. Isótopos de estroncio en calcáreos del noreste patagónico: resultados preliminares. Rev. la Asoc. Geol. Argent. 71, 526–536.
von Gosen, W., 2002. Polyphase structural evolution in the northeastern segment of the North Patagonian Massif (southern Argentina). J. S. Am. Earth Sci. 15, 591–623. http://dx.doi.org/10.1016/S0895-9811(02)00111-6.
von Gosen, W., 2003. Thrust tectonics in the North Patagonian Massif (Argentina): implications for a Patagonia plate. Tectonics 22 (1005). http://dx.doi.org/10.1029/2001TC901039.
von Gosen, W., McClelland, W.C., Loske, W., Martínez, J.C., Prozzi, C., 2014. Geochronology of igneous rocks in the Sierra Norte de Córdoba (Argentina): implications for the Pampean evolution at the western Gondwana margin. Lithosphere 6, 277–300. http://dx.doi.org/10.1130/l344.1.
Walker, J., Geissman, J., Bowring, S., Babcock, L., compilers, 2012. Geologic Time Scale v. 4.0. Geological Society of America.
Zambrano, J.J., 1980. Comarca de la cuenca cretácica de Colorado. In: Turner, J.C.M. (Ed.). Geología Regional Argentina. Academia Nacional de Ciencias, Córdoba, 1933-1070.
Zanettini, J.C., 1981. La Formación Sierra Grande (provincia de Río Negro). Rev. la Asoc. Geol. Argent. 36, 160–179.
Zappetini, E.O., Chernicoff, C.J., Santos, J.O.S., Mc Naughton, N.J., 2010. Los esquistos neoproterozoicos de Santa Helena, Provincia de La Pampa, Argentina: edades U-Pb shrimp, composición isotópica de hafnio e implicancias geodinámicas. Rev. la Asoc. Geol. Argent. 66, 21–37.